JOURNAL OF COMPUTATIONAL PHYSICS **133,** 235–255 (1997)
ARTICLE NO. CP975649

# Wavenumber-Extended High-Order Upwind-Biased Finite-Difference Schemes for Convective Scalar Transport

Yuguo Li

*CSIRO Division of Building, Construction and Engineering, Highett, Victoria 3190, Australia*

Received February 13, 1996; revised August 12, 1996

This paper proposes some new wavenumber-extended high-order upwind-biased schemes. The dispersion and dissipation errors of upwind-biased finite-difference schemes are assessed and compared by means of a Fourier analysis of the difference schemes. Up to 11th-order upwind-biased schemes are analyzed. It is shown that both the upwind-biased scheme of order $2N-1$ and the corresponding centered differencing scheme of order $2N$ have the same dispersion characteristics; thus the former can be considered to be the latter plus a correction that reduces the numerical dissipation. The new second-order wavenumber-extended scheme is tested and compared with some well-known schemes. The range of wavenumbers that are accurately treated by the upwind-biased schemes is improved by using additional constraints from the Fourier analysis to construct the new schemes. The anisotropic behavior of the dispersion and dissipation errors is also analyzed for both the conventional and the new wavenumber-extended upwind-biased finite-difference schemes. 

## 1. INTRODUCTION

An inherent limitation of any numerical method is that any wavenumber $k$ greater than $\pi/\Delta x$ on a uniform mesh cannot be resolved, where $\Delta x$ is the mesh size. In many flow situations, such as those close to discontinuities, high wavenumbers exist inherently which cause not only errors in the solution, but also numerical instability. Upwind finite-difference methods are one possible way of introducing numerical dissipation into the solution to damp high-wavenumber components. However, the numerical (artificial) dissipation may exceed the physical diffusion, especially for high Reynolds number flows. This suggests that the upwind schemes should be carefully designed to produce suitable numerical dissipation. There has been a great effort in developing second-order and third-order schemes, e.g., [1–3], and oscillation-free or monotone total variation diminishing (TVD) high-order schemes [4, 5] to reduce the numerical dissipation. In addition, the numerical dissipation may also need to be anisotropic, as the flow behavior is generally not isotropic.

Use of high-order upwind finite-difference schemes in turbulent fluid flow simulations has increased in the past decade as they provide less numerical dissipation and do not require a kinetic energy conservation property to control the aliasing error [6]. In general, although the high-order upwind schemes cannot offer the same resolution characteristics as spectral methods, they are computationally more efficient and robust and can be easily implemented in complex geometries. Following Lele [7], resolution (characteristics) in this paper means the accuracy of numerical representation of the solution over the full range of length scales that are resolvable on a mesh. Numerical spatial resolution has also been improved remarkably in the past decade as a result of the development of larger and faster computers, and has resulted in additional popularity of high-order schemes. Rai and Moin [6] revisited a finite-difference method for a direct simulation of fully developed turbulent channel flow and presented a fifth-order upwind-biased scheme [8]. This fifth-order scheme was evaluated by Tamamidis and Assanis [9] against the second-order fully upwind scheme of Warming and Beam [1] and the second-order QUICK scheme of Leonard [3]. The three schemes were applied to turbulent flow simulation with a $k-\varepsilon$ turbulence model. The fifth-order scheme was found to be superior to the other two schemes tested. Kawamura and Kuwahara [10] formulated a third-order upwind scheme using a five-point stencil with asymmetrical coefficients. The authors claimed that the scheme with numerical diffusion of fourth-order-derivative type can be used directly to model turbulent flows.

Finite-difference and finite-volume methods using high-order upwinding schemes have become some of the most commonly used methods in current computational fluid dynamics (CFD) application codes. Further development of high-order upwind schemes is important as there is a need to control the numerical dissipation and to improve the numerical solution accuracy. In this paper, upwind-biased schemes up to 11th order are analyzed. If the resolution is sufficient, a high-order scheme may be beneficial from the point of view of accuracy. It is not the purpose here to suggest that high-order schemes such as 11th-order upwind schemes can or should be used in flow simulations,



0021-9991/97 $25.00

but rather to document, analyze, and improve these schemes and to provide numerical modelers with alternative numerical schemes. As discussed later, the quality of a finite-difference scheme cannot be ranked by the order of Taylor truncation alone. This is particularly important for time-dependent flows. It should be emphasized that sufficient numerical spatial resolution is required to achieve the performance of a high-order scheme. Otherwise, the well-known Runge phenomena may occur.

Compared to spectral methods, the major shortcoming of the conventional finite-difference schemes is their lower accuracy in resolution. An extended-wavenumber method was suggested by Vichnevetsky and De Schutter [11] to maximize the range of wavenumbers that a finite-difference scheme can represent. This method was applied by Lele [7] for improvement of the resolution characteristics of compact finite-difference schemes. The resolution characteristics were greatly improved, and the new schemes are said to have spectral-like behavior by Lele. Zingg and Lomax [12] applied the same method for constructing finite-difference schemes on triangular grids. This method will be used here to develop wavenumber-extended upwind-biased schemes. The second- or fourth-order wavenumber-extended upwind-biased schemes developed in this paper provide some alternatives with better resolution characteristics for replacing the conventional second- or third-order upwind schemes in finite-difference and finite-volume simulations of practical time-dependent flows.

There are at least two other important aspects to be considered when developing high-order finite-difference schemes. The first is the robustness of their implementation. Rai and Moin [6] claimed that the upwind-biased schemes are extremely robust. There has been a considerable effort in the literature to establish reliable ways of implementing these schemes in finite-difference and finite-volume codes. For example, the implementation of the well-known QUICK schemes has been discussed in [13]. It has been shown by many authors that the deferred correction procedure of Khosla and Rubin [14] is very reliable and easy for implementation of high-order finite-difference schemes [9, 15]. In the deferred correction method, the high-order upwind scheme is considered a first-order upwind scheme with some correction terms to improve its formal accuracy. The correction terms are treated explicitly in its implementation. It is expected that the deferred correction method described in detail in [15] could be used for the schemes developed in this paper.

The second aspect to be considered when developing high-order schemes lies in the treatment of near-boundary grid points, as there is not a sufficient number of grid points for straightforward implementation of the high-order schemes. The most conventional method of boundary point treatment is to apply lower-order schemes near the boundaries. It was found by many authors that the results with lower-order schemes near the boundary are far superior to those obtained by the lower-order schemes everywhere [6, 15]. However, the overall accuracy decreases compared to what is expected from a higher-order scheme. Gustafsson [16] predicted that the boundary conditions should be at least of an order of $N - 1$ in order to retain an $N$th-order global accuracy. Some higher-order boundary conditions and their stability are discussed extensively in [17, 18], for example. These two aspects will not be discussed further in this paper.

It should also be mentioned that despite the damping at the high-wavenumber range, the high-order upwind-biased schemes developed in this paper still suffer from a lack of positivity in regions of high variable gradients. Among many possibilities, the well-known FCT technique [19] can be used to eliminate the numerical oscillations, as demonstrated extensively by Li and Rudman [20].

The emphasis of this work is to apply Fourier analysis to analyze in detail the high-order upwind-biased finite-difference schemes and develop new upwind-biased schemes with better resolution characteristics. As compact (implicit) schemes and their wavenumber-extended counterparts have been treated extensively by Lele [7], and explicit centered differencing schemes by Tam and Webb [21], the focus here will be on explicit upwind-biased schemes. The upwind-biased schemes without wavenumber extension will be presented for the first derivatives of up to 11th order and those with wavenumber extension of up to 8th order. A detailed analysis of anisotropic behavior of these schemes will also be presented. All the schemes are documented in detail in Appendixes 1 and 3.

## 2. FORMULATION OF HIGH-ORDER UPWIND-BIASED SCHEMES

### 2.1. *General Formulation*

It is well known that the finite-difference approximation of the first derivative of a dependent variable, $\phi$, can be expressed as a linear combination of the given variable values at some discrete grid points. In this paper, we are interested in those schemes formulated by using the Taylor series truncation.

For simplicity, consider a uniform grid with index $j$. For a $2N + 1$ point stencil ($j$, $j \pm 1$, ..., $j \pm N$), $x_{j\pm n} = \pm n\Delta x$ at node $j \pm n$, and $x_j = 0$ at node $j$. The variable values $\phi_{j\pm n} = \phi(x_{j\pm n})$ are given.

The following generalized formulation is proposed. This formulation will also be used later for Fourier analysis of the schemes,

$$\left[\frac{\partial \phi}{\partial x}\right]_j = \frac{1}{\Delta x}\left(\sum_{n=1}^{N} a_{-n}\phi_{j-n} + a_0\phi_j + \sum_{n=1}^{N} a_n\phi_{j+n}\right) + O(\Delta x^M), \tag{1}$$

where the coefficients $a_0$, $a_n$, and $a_{-n}$ ($n = 1, 2, ..., N$) are to be determined (for the conventional schemes) by matching the Taylor series coefficients of various orders. $M$ is the order of truncation error of the finite-difference scheme, which is related to the first unmatched coefficient. Later in this paper, it is proposed that additional constraints from the Fourier analysis of the scheme can be introduced to determine the coefficients. To clarify the scheme terminology and concepts, some conventional schemes derived from the Taylor series truncation are briefly reviewed below.

Using a $2N + 1$ point stencil in Eq. (1), the Taylor series expansions for $\phi_{j\pm n}$ are

$$\phi_{j\pm n} = \sum_{k=0}^{\infty} \frac{(\pm n\Delta x)^k}{k!} \left(\frac{\partial^k \phi}{\partial x^k}\right)_j. \tag{2}$$

There are many different schemes that can be derived from the general formulation (1). These schemes can be classified as

- fully upwind schemes
- partial upwind schemes, Type 1
- partial upwind schemes, Type 2
- centered difference schemes.

### 2.2. *Centered Difference Schemes*

The use of the entire $2N + 1$ point stencil with symmetrical coefficients ($a_{-n} = -a_n$) would result in a *centered difference scheme* of order $2N$, which is nondissipative.

The constraints in deriving the centered difference schemes are a system of $2N + 1$ linear equations:

$$\begin{aligned}
&\sum_{n=1}^{N} (a_n + a_{-n}) + a_0 = 0 \\
&\sum_{n=1}^{N} n(a_n - a_{-n}) = 1 \\
&\sum_{n=1}^{N} \frac{n^k}{k!}(a_n + a_{-n}) = 0, \qquad k = 2, 4, 6, ..., 2N \\
&\sum_{n=1}^{N} \frac{n^k}{k!}(a_n - a_{-n}) = 0, \qquad k = 3, 5, 7, ..., 2N - 1.
\end{aligned} \tag{3}$$

### 2.3. *Fully Upwind Schemes*

To control aliasing error, it was suggested that the upwind schemes be used, which can damp the high-frequency components, e.g., [6]. In a *fully upwind scheme*, only values at those upwind nodes are used in the formulation (1). The formulation (1) becomes

$$\begin{aligned}
\left[\frac{\partial \phi}{\partial x}\right]_j &= \frac{1}{\Delta x}\left(\sum_{n=1}^{N} a_{-n}\phi_{j-n} + a_0\phi_j\right) + O(\Delta x^N); \quad u_j > 0 \\
\left[\frac{\partial \phi}{\partial x}\right]_j &= \frac{1}{\Delta x}\left(\sum_{n=1}^{N} a_n\phi_{j+n} + a_0\phi_j\right) + O(\Delta x^N); \quad u_j < 0.
\end{aligned} \tag{4}$$

The scheme will be $N$th order.

For example, when $N = 2$, the familiar second-order fully upwind scheme [1] is obtained:

$$\begin{aligned}
\left[\frac{\partial \phi}{\partial x}\right]_j &= \frac{1}{2\Delta x}(\phi_{j-2} - 4\phi_{j-1} + 3\phi_j) + O(\Delta x^2); \quad u_j > 0 \\
\left[\frac{\partial \phi}{\partial x}\right]_j &= \frac{1}{2\Delta x}(-3\phi_j + 4\phi_{j+1} - \phi_{j+2}) + O(\Delta x^2); \quad u_j < 0.
\end{aligned} \tag{5}$$

### 2.4. *Partial Upwind Schemes, Type 1*

When $N \geq 2$, *partial upwind schemes* (*type 1*) can be formulated by using some additional but not all downwind points in the approximation, i.e.,

$$\begin{aligned}
\left[\frac{\partial \phi}{\partial x}\right]_j &= \frac{1}{\Delta x}\left(\sum_{n=1}^{N} a_{-n}\phi_{j-n} + a_0\phi_j + \sum_{n=1}^{M} a_n\phi_{j+n}\right); \quad u_j > 0 \\
\left[\frac{\partial \phi}{\partial x}\right]_j &= \frac{1}{\Delta x}\left(\sum_{n=1}^{M} a_{-n}\phi_{j-n} + a_0\phi_j + \sum_{n=1}^{N} a_n\phi_{j+n}\right); \quad u_j < 0,
\end{aligned} \tag{6}$$

where $M < N$.

When $N = 2$, the general relation (6) becomes

$$\begin{aligned}
\left[\frac{\partial \phi}{\partial x}\right]_j &= \frac{1}{\Delta x}(a_{-2}\phi_{j-2} + a_{-1}\phi_{j-1} + a_0\phi_j + a_1\phi_{j+1}); \quad u_j > 0 \\
\left[\frac{\partial \phi}{\partial x}\right]_j &= \frac{1}{\Delta x}(a_{-1}\phi_{j-1} + a_0\phi_j + a_1\phi_{j+1} + a_2\phi_{j+2}); \quad u_j < 0.
\end{aligned} \tag{7}$$

This is a subfamily of the five-point partial upwind schemes. Two well-known five-point partial upwind schemes are the third-order upwind-biased scheme [6]

$$\begin{aligned}
\left[\frac{\partial \phi}{\partial x}\right]_j &= \frac{1}{6\Delta x}(\phi_{j-2} - 6\phi_{j-1} + 3\phi_j + 2\phi_{j+1}) + O(\Delta x^3); \\
&\qquad\qquad u_j > 0 \\
\left[\frac{\partial \phi}{\partial x}\right]_j &= \frac{1}{6\Delta x}(-2\phi_{j-1} - 3\phi_j + 6\phi_{j+1} - \phi_{j+2}) + O(\Delta x^3); \\
&\qquad\qquad u_j < 0
\end{aligned} \tag{8}$$

and Leonard's second-order QUICK scheme [3]

$$\left[\frac{\partial\phi}{\partial x}\right]_j = \frac{1}{8\Delta x}(\phi_{j-2} - 7\phi_{j-1} + 3\phi_j + 3\phi_{j+1}) + O(\Delta x^2); \quad u_j > 0$$
$$\left[\frac{\partial\phi}{\partial x}\right]_j = \frac{1}{8\Delta x}(-3\phi_{j-1} - 3\phi_j + 7\phi_{j+1} - \phi_{j+2}) + O(\Delta x^2); \quad u_j < 0. \tag{9}$$

The family of schemes (7) has received special attention in CFD. The third-order upwind-biased schemes and the second-order QUICK scheme of Leonard can be generalized as [22]

$$\left[\frac{\partial\phi}{\partial x}\right]_j = \frac{1}{2\Delta x}(\phi_{j+1} - \phi_{j-1}) - \frac{q}{\Delta x}(\phi_{j+1} - 3\phi_j + 3\phi_{j-1} - \phi_{j-2}); \quad u_j > 0$$
$$\left[\frac{\partial\phi}{\partial x}\right]_j = \frac{1}{2\Delta x}(\phi_{j+1} - \phi_{j-1}) - \frac{q}{\Delta x}(-\phi_{j-1} + 3\phi_j - 3\phi_{j+1} + \phi_{j+2}); \quad u_j > 0. \tag{10}$$

For second-order centered differencing, $q = 0$, for the second-order fully upwind scheme, $q = 0.5$, for Leonard's second-order QUICK scheme, $q = 1/8$, and for the third-order upwind-biased scheme, $q = 1/6$. The coefficient $q$ can also be so chosen that it depends on the local Peclet number to minimize the potential oscillations by minimizing the remote-node coefficients, while maintaining the positive neighbor-node coefficients in the finite-volume formulation; see [20]. An expression analogous to Eq. (10) on nonuniform grids was formulated by Li and Rudman [20].

### 2.5. *Partial Upwind Schemes, Type 2*

The use of the entire $2N + 1$ point stencil with asymmetrical coefficients can also result in a *partial upwind scheme* (*type 2*), and the upwinding effect is taken into account by using larger absolute coefficients for upwinding points, i.e.,

$$|a_{-N}| > |a_N|; \quad u_j > 0$$
$$|a_{-N}| < |a_N|; \quad u_j < 0. \tag{11}$$

Kawamura and Kuwahara's third-order partial upwind scheme [10] belongs to this family for $N = 2$:

$$\left[\frac{\partial\phi}{\partial x}\right]_j = \frac{1}{6\Delta x}(2\phi_{j-2} - 10\phi_{j-1} + 9\phi_j - 2\phi_{j+1} + \phi_{j+2}) + O(\Delta x^3); \quad u_j > 0$$
$$\left[\frac{\partial\phi}{\partial x}\right]_j = \frac{1}{6\Delta x}(-\phi_{j-2} + 2\phi_{j-1} - 9\phi_j + 10\phi_{j+1} - 2\phi_{j+2}) + O(\Delta x^3); \quad u_j < 0. \tag{12}$$

### 2.6. *Upwind-Biased Schemes*

In this paper, the focus is on a particular class of the partial upwind schemes (type 1), in which $M = N - 1$ in the general formulation (6)—we reserve the name of *upwind-biased schemes* for this class of schemes. The upwind-biased schemes provide the maximum formal order of accuracy for partial upwind schemes of Type 1 when $N$ is chosen. Up to fifth-order upwind-biased schemes have been used by Rai and Moin [6] for direct simulation of turbulent channel flow and were found to be robust. In this paper, up to 11th-order accurate upwind-biased schemes are formulated. It should be mentioned that the first-order upwind scheme ($N = 1$) is a special case of the upwind-biased schemes and is also a fully upwind scheme (i.e., $N = 1$ in Eq. (1)). As can be seen from Appendix 1, the upwind-biased schemes share similar patterns in some of their coefficients, namely that the denominator is $N!$ for $N$th-order upwind-biased schemes, and the coefficient for $\phi_{j+1}$ is $N!$ when $u_j < 0$, and $\phi_{j-1}$ is $-N!$ when $u_j > 0$.

The constraints in deriving these schemes are

$$a_N = 0; \quad u_j > 0$$
$$a_{-N} = 0; \quad u_j < 0$$
$$\sum_{n=1}^{N}(a_n + a_{-n}) + a_0 = 0$$
$$\sum_{n=1}^{N} n(a_n - a_{-n}) = 1$$
$$\sum_{n=1}^{N}\frac{n^k}{k!}(a_n + a_{-n}) = 0, \quad k = 2, 4, 6, ..., 2N - 2$$
$$\sum_{n=1}^{N}\frac{n^k}{k!}(a_n - a_{-n}) = 0, \quad k = 3, 5, 7, ..., 2N - 1. \tag{13, 14}$$

It can be seen from (14) that both the upwind-biased scheme of order $2N - 1$ and the corresponding centered difference scheme of order $2N$ share the same constraints on $a_n - a_{-n}$, i.e.,

$$\sum_{n=1}^{N} n(a_n - a_{-n}) = 1$$
$$\sum_{n=1}^{N} \frac{n^k}{k!}(a_n - a_{-n}) = 0, \quad k = 3, 5, 7, ..., 2N-1. \tag{15}$$

The total number of the equations in (15) is $N$ and the total number of variables $(a_n - a_{-n})$ is also $N$. Thus, the solutions of equations (15) are the same for both the upwind-biased scheme and the corresponding centered difference scheme. This provides an important characteristic for the upwind-biased schemes as compared to the corresponding centered differencing schemes in their dispersion characteristics. It will be shown later that the upwind-biased schemes have the same dispersion characteristics as the corresponding centered differencing scheme. Thus, the upwind-biased scheme of order $2N-1$ can be considered a correction to the centered difference scheme of order $2N$ that adds some numerical dissipation.

If $\partial\phi/\partial x$ represents the exact first derivative and $[\partial\phi/\partial x]_N^U$ represents the upwind-biased finite-difference formulation of $N$th order, Taylor expansion analysis shows that for $u_j > 0$

$$\frac{\partial\phi}{\partial x} = \left[\frac{\partial\phi}{\partial x}\right]_1^U - \frac{1}{2}\Delta x \frac{\partial^2\phi}{\partial x^2} + O(\Delta x^2)$$
$$\frac{\partial\phi}{\partial x} = \left[\frac{\partial\phi}{\partial x}\right]_3^U + \frac{1}{12}\Delta x^3 \frac{\partial^4\phi}{\partial x^4} + O(\Delta x^4)$$
$$\frac{\partial\phi}{\partial x} = \left[\frac{\partial\phi}{\partial x}\right]_5^U - \frac{1}{60}\Delta x^5 \frac{\partial^6\phi}{\partial x^6} + O(\Delta x^6) \tag{16}$$
$$\frac{\partial\phi}{\partial x} = \left[\frac{\partial\phi}{\partial x}\right]_7^U + \frac{1}{280}\Delta x^7 \frac{\partial^8\phi}{\partial x^8} + O(\Delta x^8)$$
$$\frac{\partial\phi}{\partial x} = \left[\frac{\partial\phi}{\partial x}\right]_9^U - \frac{1}{1260}\Delta x^9 \frac{\partial^{10}\phi}{\partial x^{10}} + O(\Delta x^{10}).$$

## 3. FOURIER ANALYSIS OF 1D DISCRETIZATION ERROR

The above truncation error analysis does not represent all the characteristics of a scheme. Because many fluid flows exhibit wave-like motions, a Fourier analysis of a scheme can provide additional information about its resolution characteristics. The question is whether a scheme represents the full range of length scales on a given mesh. The classical Fourier analysis of numerical discretization schemes has been used by many authors, e.g., [23]. Inspired by Lele's work, additional constraints provided by the Fourier analysis are used here to improve the resolution characteristics of the high-order upwind-biased schemes that are formulated in Section 2.6.

### 3.1. *Modified Wavenumber*

Over the stencil domain $(-L/2, L/2)$, we assume that the dependent variable $\phi$ is periodic, $\Delta x = L/2N$. A Fourier representation of $\phi(x)$ in the interval $[j-N, j+N]$ is

$$\phi(x) = \sum_{l=-N}^{N} \hat{\phi}_l e^{(2\pi i l x/L)}, \tag{17}$$

where $i = \sqrt{-1}$ is the imaginary unit. Be aware that $\phi(x)$ is real-valued,

$$\hat{\phi}_l = \hat{\phi}^*_{-l}$$
$$\hat{\phi}_0 = \hat{\phi}^*_0, \tag{18}$$

where * is the complex conjugate.

By introducing a scaled wavenumber $k_l$ for $0 \le l \le N$ and a scaled coordinate $\bar{x}$

$$k_l = \frac{2\pi l \Delta x}{L} = \frac{\pi l}{N}$$
$$\bar{x} = \frac{x - x_j}{\Delta x} \tag{19}$$

Eq. (17) becomes

$$\phi(\bar{x}) = \sum_{l=0}^{N} \hat{\phi}_l e^{ik_l\bar{x}}. \tag{20}$$

The exact first derivative of the variable $\phi$ is

$$\frac{\partial\phi}{\partial x} = \sum_{l=0}^{N} ik_l \hat{\phi}_l e^{ik_l\bar{x}}. \tag{21}$$

The differencing scheme (1) with the scaled coordinate can be written as

$$\left[\frac{\partial\phi}{\partial\bar{x}}\right]_j = \sum_{n=1}^{N} a_{-n}\phi_{j-n} + a_0\phi_j + \sum_{n=1}^{N} a_n\phi_{j+n} + O(\Delta\bar{x}^M), \tag{22}$$

where

$$\bar{x}_{j\pm n} = \pm n, \quad \bar{x}_j = 0$$
$$\phi_{j\pm n}(\bar{x}_{j\pm n}) = \sum_{l=0}^{N} \hat{\phi}_l e^{ik_l\bar{x}_{j\pm n}} = \sum_{l=0}^{N} \hat{\phi}_l e^{\pm ink_l} \tag{23}$$
$$\phi_j(\bar{x}_j) = \sum_{l=0}^{N} \hat{\phi}_l.$$

Thus, the numerical approximation of the first derivative of the variable $\phi$ is

$$\left[\frac{\partial \phi}{\partial \bar{x}}\right]_j = \sum_{l=0}^{N}\left[\sum_{n=1}^{N} a_{-n}e^{-ik_l n} + a_0 + \sum_{n=1}^{N} a_n e^{ink_l}\right] = \sum_{l=0}^{N}\left[\sum_{n=1}^{N}((a_n + a_{-n})\cos(nk_l)) + a_0 + i\sum_{n=1}^{N}((a_n - a_{-n})\sin(nk_l))\right]\hat{\phi}_l. \tag{24}$$

Comparing the exact solution (21) to the approximation (24), we see that the wavenumber $k$ in the solution (21) is modified in the approximation (24). If we write the approximate solution (24) as

$$\left[\frac{\partial \phi}{\partial x}\right]_j = \sum_{l=0}^{N} ik^*\hat{\phi}_l e^{ik_l \bar{x}_j}, \tag{25}$$

where $k^*$ is the modified wavenumber,

$$k^* = \sum_{n=1}^{N}[(a_n - a_{-n})\sin(nk_l)] - i\left(\sum_{n=1}^{N}[(a_n + a_{-n})\cos(nk_l)] + a_0\right). \tag{26}$$

Generally, the modified wavenumber $k^*$ is a complex function. The real part $k_r^*$ and the imaginary part $k_i^*$ are associated with the dispersion error (phase error) and the dissipative error (amplitude error), respectively, as will be shown in the next section.

$$k_r^* = \sum_{n=1}^{N}[(a_n - a_{-n})\sin(nk_l)]$$
$$k_i^* = \sum_{n=1}^{N}[(a_n + a_{-n})\cos(nk_l)] + a_0. \tag{27}$$

Due to the symmetry of coefficients ($a_n = -a_{-n}$), we have $k_i^* = 0$ for all the centered difference schemes. Thus, all the centered difference schemes are nondissipative.

### 3.2. *Dispersion Error and Dissipation Error*

The above definition of the dispersion error and the dissipation error can be easily understood by examining the exact solution of the advection equation with diffusion and the numerical solution of the advection equation.

Applying the above finite-difference schemes (1) in the advection equation

$$\frac{\partial \phi}{\partial t} + \frac{\partial \phi}{\partial \bar{x}} = 0 \tag{28}$$

we obtain

$$\left[\frac{d\hat{\phi}_l}{dt}\right]_j = -(iuk_r^* + uk_i^*)\hat{\phi}_l. \tag{29}$$

Thus

$$\hat{\phi}_l(t) = \hat{\phi}_l(0)e^{-uik_r^* t}e^{-uk_i^* t}. \tag{30}$$

For the advection equation with diffusion

$$\frac{\partial \phi}{\partial t} + u\frac{\partial \phi}{\partial \bar{x}} = \mu\frac{\partial^2 \phi}{\partial \bar{x}^2}. \tag{31}$$

Assume that the initial condition and solution form are

$$\phi(\bar{x}, t) = \sum_{l=0}^{N}\hat{\phi}_l(t)e^{ik_l\bar{x}}. \tag{32}$$

Equation (31) becomes

$$\frac{d\hat{\phi}_l}{dt} = -(iuk_l + \mu k_l^2)\hat{\phi}_l. \tag{33}$$

The solution of Eq. (31) with initial condition (32) is

$$\hat{\phi}_l(t) = \hat{\phi}_l(0)e^{-iuk_l t}e^{-\mu k_l^2 t}. \tag{34}$$

Comparing solutions (34) and (30), it is obvious $k_r^*$ is a modified wavenumber and $k_i^*$ is associated with numerical dissipation. The following numerical dissipation can be defined:

$$\mu^* = u\frac{k_i^*}{k_l^2}. \tag{35}$$

This definition provides a possible way of studying how the numerical dissipation varies with wavenumber.

An alternative way of studying the numerical dispersion to the use of the real part of the modified wavenumber is to use the concept of numerical phase speed. If the approximate solution (30) is written as

$$\hat{\phi}_l(t) = \hat{\phi}_l(0)e^{-iu^* k_l t}e^{-uk_i^* t}, \tag{36}$$

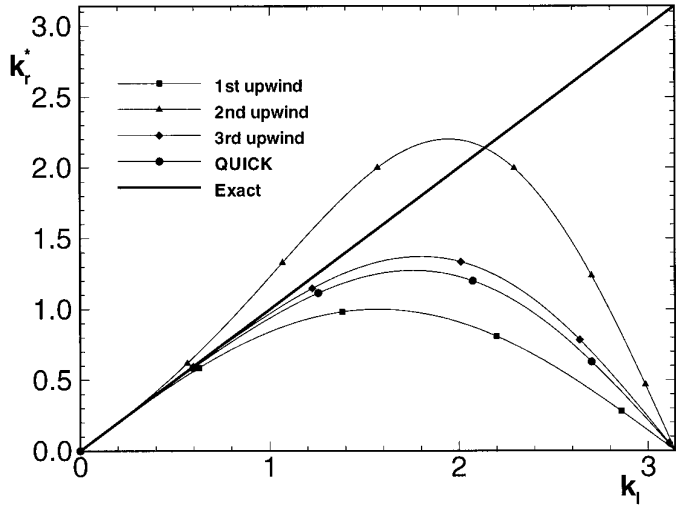


**FIG. 1.** The numerical dispersion errors as indicated by the real part of the modified wavenumber versus wavenumber for some conventional finite-difference schemes, including the first-order upwind scheme, second-order fully upwind scheme, QUICK scheme, and third-order upwind-biased scheme.

where $u^*$ is defined as the numerical phase speed, it is easy to show that

$$\frac{u^*}{u} = \frac{k_r^*}{k_l}. \tag{37}$$

Thus, the dispersion error resulting from a finite-difference scheme can also be seen from the modified phase speed $u^*$. The numerical phase speeds vary for different wavenumbers.

### 3.3. *Analysis of Some Conventional Schemes*

Figure 1 shows the real part of the modified wavenumber versus wavenumber for the first-order upwind scheme, second-order fully upwind scheme (Eq. (5)), the QUICK scheme (Eq. (9)), and the third-order upwind-biased scheme (Eq. (8)). The diagonal solid line represents the dispersion characteristics of the exact solution. It can be seen that the higher-order schemes generally exhibit better dispersion characteristics than lower-order schemes. The second-order fully upwind scheme enters the upper triangle. This indicates that the numerical phase speeds for wavenumbers in the range (0.3, 2.1) are faster than the real phase speed for the second-order fully upwind scheme. For other schemes in Fig. 1, the numerical phase speeds are slower than or equal to the real phase speed.

The fact that numerical phase speeds can be different from the real phase speed gives rise to the familiar oscillations around discontinuities [24]. Li and Rudman [20] studied the rotation of a scalar cone and observed that oscillations occur in front of the cone for the second-order fully upwind scheme and behind the cone for QUICK. Perspective plots of the predicted results of a scalar cone 10 units high after one full rotation are shown in Fig. 2 for the two schemes. Figure 1 shows that this difference is due to the waves in the range (0.3, 2.1) traveling slower for the QUICK scheme and faster for the second-order fully upwind scheme.

The imaginary part of the modified wavenumber versus wavenumber for these conventional schemes are shown in Fig. 3. The QUICK scheme (Eq. (9)) and the third-order upwind-biased scheme (Eq. (8)) are able to provide very small numerical dissipation for a much wider low-wavenumber range than the first-order upwind scheme. At the

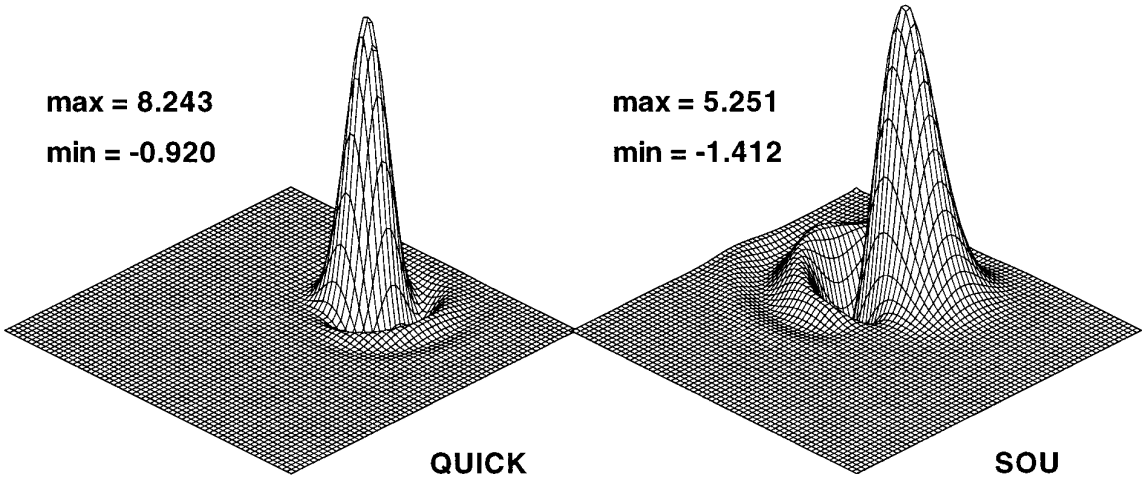


**FIG. 2.** Perspective plots of the predicted results of a scalar cone 10 units high after one full rotation with the QUICK scheme (left) and the second-order fully upwind scheme (SOU) (right). The maximum Courant number used is 0.09. The grid is 64 × 64. Rotation is counterclockwise.

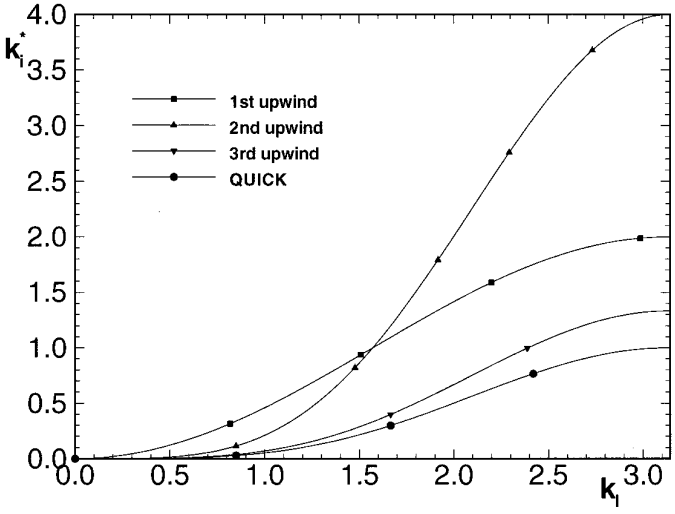


**FIG. 3.** The numerical dissipation errors as indicated by the imaginary part of the modified wavenumber versus wavenumber for some conventional finite-difference schemes, including the first-order upwind scheme, second-order fully upwind scheme, QUICK scheme, and third-order upwind-biases scheme.

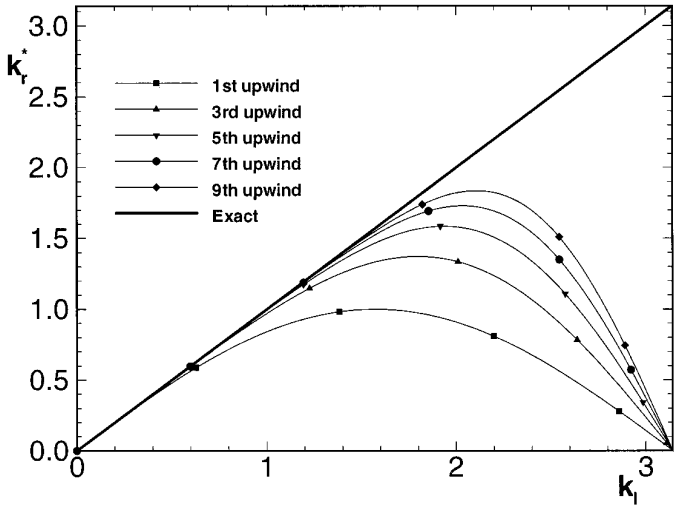


**FIG. 4.** The numerical dispersion errors as indicated by the real part of the modified wavenumber versus wavenumber for different upwind-biased finite-difference schemes.

low-wavenumber range, the second-order fully upwind scheme performs much better than the first-order scheme. However, it introduces much larger dissipation for the high-wavenumber range, which can be of some advantage if artificial numerical dissipation is needed in the high-wavenumber range, as explained in the Introduction.

The accuracy assessment above of the second-order fully upwind scheme and the second-order QUICK scheme based on the Fourier analysis agrees well with the numerical assessment in [20]. This illustrates that the Fourier analysis is a powerful tool for finite-difference schemes. In the next section, a Fourier analysis of Eq. (27) will be used to construct some new finite-difference schemes.

## 4. WAVENUMBER-EXTENDED SCHEMES

### 4.1. *Fourier Analysis of Upwind-Biased Schemes*

In Figs. 4 and 5, the real and the imaginary parts $k_r^*$ and $k_i^*$ are shown for different upwind-biased schemes which are formulated in Section 2.6 and summarized in Appendix 1.

Generally, the higher the order of an upwind-biased scheme, the better its resolution characteristics will be. The higher-order upwind-biased schemes generally introduce much less (or no) numerical dissipation for the low-wavenumber range. For problems in which numerical dissipation is needed for the high-wavenumber range, one might argue that these schemes introduce numerical dissipation at just the right place, although the level of the numerical dissipation may not be ideal, depending on the problem. Generally, the higher the order of a scheme, the less the numerical dissipation in Fig. 5. If no dissipation is needed, then upwind schemes are not a suitable option, and centered difference schemes should be considered.

It is easy to prove that the upwind-biased scheme of order $2N-1$ has the same dispersion characteristics in Fourier space as that of the centered difference scheme of order $2N$. This is because the same constraints on $(a_n - a_{-n})$ are used in both the upwind-biased scheme of order $2N-1$ and the corresponding centered difference scheme of order $2N$. As can be seen from Eq. (27), the dependence

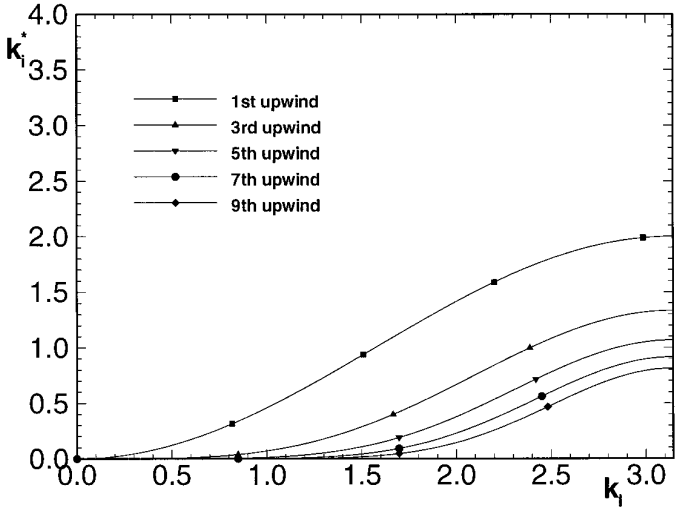


**FIG. 5.** The numerical dissipation errors as indicated by the imaginary part of the modified wavenumber versus wavenumber for different upwind-biased finite-difference schemes.

of the dispersion characteristics on the scheme coefficients is only $(a_n - a_{-n})$. It should also be mentioned that the centered differencing schemes are nondissipative; i.e., $k_i^* = 0$. Thus, in the Fourier space, the upwind-biased schemes of order $2N - 1$ can be considered as resulting from the corresponding centered difference scheme of order $2N$ with the addition of numerical dissipation.

### 4.2. *Development of Wavenumber-Extended Schemes*

The general expression of the modified wavenumber (Eq. (27)) can be used to provide some additional constraints in constructing new upwind-biased schemes. The idea is to extend the accurate range of wavenumbers that the scheme can resolve, i.e., to extend the scheme to follow as closely as possible to the spectral resolution shown in Fig. 4. This can be done by replacing the last equations of the constraints (Eq. 14) with new constraints resulting from the Fourier analysis.

There are at least two approaches to formulating the new constraints from the Fourier analysis. Lele's wavenumber fit approach [7] is to choose a wavenumber $k_{l1}$ or several wavenumbers and fit the modified wavenumbers to the corresponding true wavenumbers. The following constraint is imposed:

$$k_r^*(k_{l1}) = k_{l1}. \tag{38}$$

$k_{l1}$ is so chosen that the resulting wavenumber-extended schemes follow the spectral resolution as close as possible. Generally, a range of possible $k_{l1}$ values is tested to choose the one which gives the best resolution performance of the resulting scheme. This process is somewhat arbitrary. Lele [7] used this approach to improve the resolution characteristics of a family of compact schemes.

The second approach is an integrated error minimization method, proposed by Tam and Webb [21]. In this method, the conditions that an integrated error is a minimum are used as the new constraints. For example, an integrated error can be defined as

$$E_{br} = \int_0^{\gamma\pi} (k_r^* - k)^2 \, dk, \tag{39}$$

where the factor $\gamma$ $(0 \le \gamma \le 1)$ defines the optimization range of wavenumbers. The conditions that $E_r$ is a minimum are

$$\frac{\partial E}{\partial a_J} = 0, \quad J = -N \text{ to } N. \tag{40}$$

In this method, the choice of the factor $\gamma$ is very important. As the scaled modified wavenumber approaches zero when the true wavenumber is $\pi$, it can be shown that a full optimization range ($\gamma = 1$) will not produce a meaningful optimized scheme. The details of the integrated error minimization method and choice of $\gamma$ used in this paper are summarized in Appendix 2.

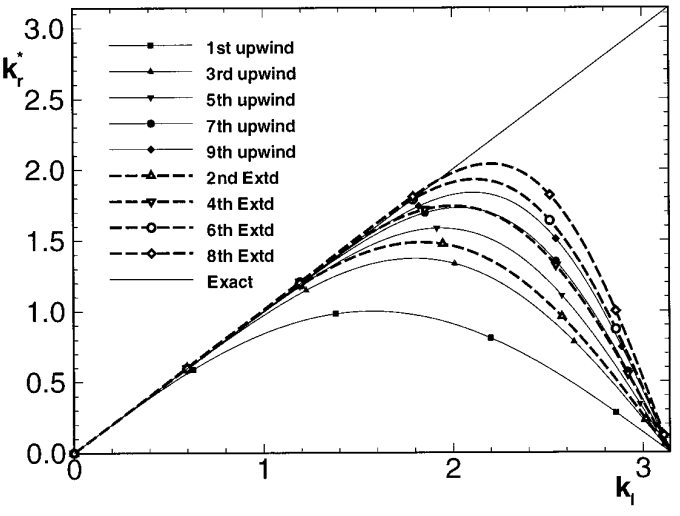


**FIG. 6.** The numerical dispersion errors as indicated by the real part of the modified wavenumber versus wavenumber for different wavenumber-extended upwind-biased finite-difference schemes.

The following constraints are used here when deriving the wavenumber-extended upwind-biased schemes:

$$\begin{aligned}
a_N &= 0; \quad u_j > 0 \\
a_{-N} &= 0; \quad u_j < 0 \\
\sum_{n=1}^{N} (a_n + a_{-n}) + a_0 &= 0 \\
\sum_{n=1}^{N} n(a_n - a_{-n}) &= 1 \\
\sum_{n=1}^{N} \frac{n^k}{k!} (a_n + a_{-n}) &= 0, \quad k = 2, 4, 6, \ldots, 2N-2 \\
\sum_{n=1}^{N} \frac{n^k}{k!} (a_n - a_{-n}) &= 0, \quad k = 3, 5, 7, \ldots, 2N-3 \\
\frac{\partial E}{\partial a_{-1}} &= 0.
\end{aligned} \tag{41}$$

The resulting new schemes are of $2N - 2$ formal order, which is one order lower than the corresponding upwind-biased schemes. However, their wavenumber resolution ranges are greatly improved. Appendix 3 documents the wavenumber-extended upwind-biased schemes developed.

The real part of the modified wavenumber $k_r^*$ for the new schemes are shown in Fig. 6. It can be seen that the resolution characteristics do not depend only on the formal

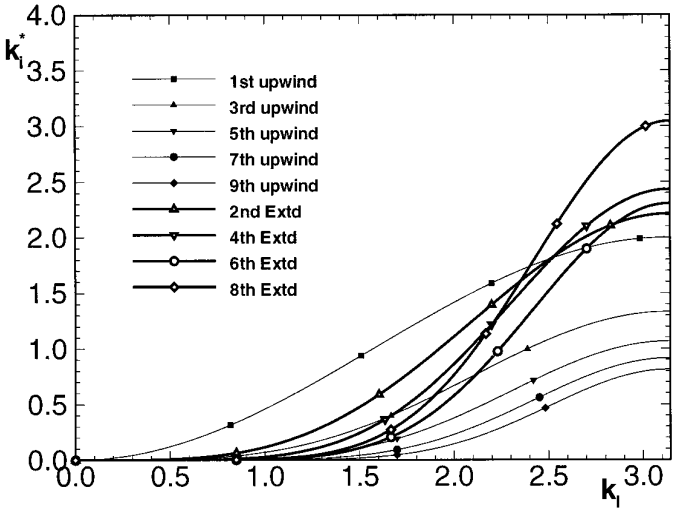


**FIG. 7.** The numerical dissipation errors as indicated by the imaginary part of the modified wavenumber versus wavenumber for different wavenumber-extended upwind-biased finite-difference schemes including a numerical dissipation constraint.

accuracy of a high-order upwind scheme. The second-order wavenumber-extended upwind scheme has a wavenumber resolution capacity almost the same as the fifth-order upwind-biased scheme. The second-order wavenumber-extended upwind scheme uses only a five-point stencil, while the fifth-order upwind-biased scheme uses a seven-point stencil. Similar conclusions can be drawn for other wavenumber-extended schemes shown in Fig. 6.

The question is, what price do we pay for the improved resolution characteristics of a wavenumber-extended upwind scheme? Figure 7 shows the imaginary part of the modified wavenumber which is associated with the dissipation error. For the wavenumber-extended schemes (order $2N - 2$) derived, there is an increase of the dissipation error in the high-wavenumber range compared to the corresponding upwind-biased scheme (order $2N - 1$). However, the increase of numerical dissipation in the low-wavenumber range is very small. It is also seen from Figs. 7 and 3 that the second-order wavenumber-extended upwind scheme provides much less numerical dissipation for the high-wavenumber range than the second-order fully upwind scheme. As discussed in the Introduction, some numerical dissipation is needed in the high-wavenumber range for some flow problems. The decision that a numerical modeler should always make is how much numerical dissipation is needed. The above wavenumber-extended upwind schemes provide some additional alternatives for adjusting numerical dissipation.

It is also possible to specify an additional constraint on the imaginary part of the modified wavenumber in the constraints (41). There are also two approaches available for introducing the additional constraint from the imaginary part of the modified wavenumber: Lele's approach and Tam and Webb's integrated error minimization approach. For demonstration purposes, Lele's approach is used for the second class of schemes. The details of applying the Tam and Webb approach for the imaginary part of the modified wavenumber are described in Appendix 2. We will reduce the formal accuracy further to $2N - 3$ by freeing one more constraint from the Taylor expansion analysis. The constraints in deriving these new wavenumber-extended schemes are

$$\begin{aligned}
a_N &= 0; \quad u_j > 0 \\
a_{-N} &= 0; \quad u_j < 0 \\
\sum_{n=1}^{N} (a_n + a_{-n}) + a_0 &= 0 \\
\sum_{n=1}^{N} n(a_n - a_{-n}) &= 1 \\
\sum_{n=1}^{N} \frac{n^k}{k!}(a_n + a_{-n}) &= 0, \quad k = 2, 4, 6, ..., 2N - 4 \\
\sum_{n=1}^{N} \frac{n^k}{k!}(a_n - a_{-n}) &= 0, \quad k = 3, 5, 7, ..., 2N - 3 \\
k_r^*(k_{l1}) &= k_{l1} \\
k_i^*(k_{l2}) &= c_2,
\end{aligned} \tag{42}$$

where the wavenumber $k_{l1}$ is so chosen that the resulting wavenumber-extended schemes follow the spectral resolution as close as possible, and the wavenumber $k_{l2}$ is so chosen that the resultant wavenumber-extended schemes have the imaginary part of the modified wavenumber at $k_{l2}$ as the specified value of $c_2$. The new schemes developed are documented in Appendix 3.

Some of the resulting schemes are shown in Figs. 8 and 9. The following values of $k_{l1}$, $k_{l2}$, and $c_2$ are used: for the third-order wavenumber-extended upwind-biased scheme 1 (3rd Extd[1]), $k_{l1} = 1.7$, $k_{l2} = 3.1$, $c_2 = 0.0$, and $N = 3$; for the third-order wavenumber-extended upwind-biased scheme 2 (3rd Extd[2]), $k_{l1} = 1.7$, $k_{l2} = 3.1$, $c_2 = 0.25$, and $N = 3$; and for the seventh-order wavenumber-extended upwind-biased scheme 1 (7th Extd[1]), $k_{l1} = 2.2$, $k_{l2} = 3.1$, $c_2 = 0.25$, and $N = 5$.

The dispersion characteristics of the new schemes in Fig. 8 are very similar to those of their counterparts in which only the dispersion range is extended in Fig. 6. A disturbing feature of these new schemes based on the constraints (42) is that the imaginary part of the modified wavenumber becomes negative for some wavenumber ranges (see Fig. 9). A stable scheme must at least have $\mu^* > 0$. Thus, these schemes may not be practically applicable to real problems.

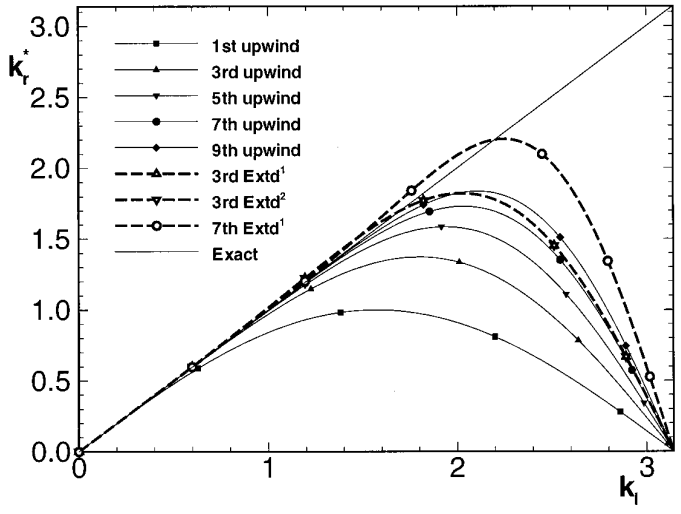


**FIG. 8.** The numerical dispersion errors as indicated by the real part of the modified wavenumber versus wavenumber for different wavenumber-extended upwind-biased finite-difference schemes including a numerical dissipation constraint.

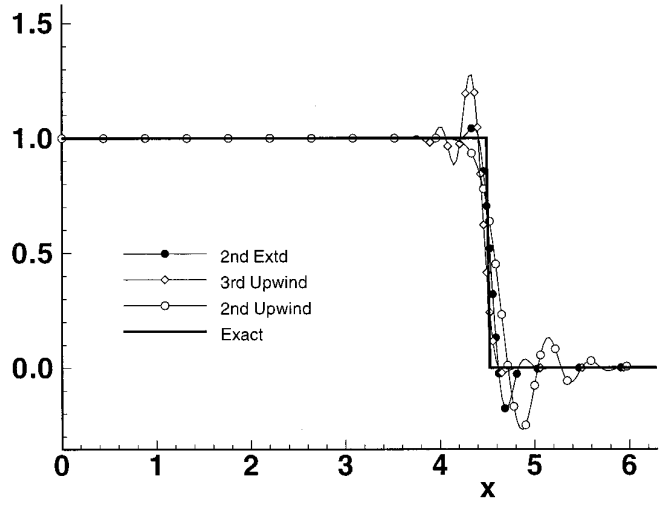


**FIG. 10.** Comparison of three schemes on the linear convection equation for a propagating discontinuity.

Thus, the schemes based on the constraints (42) are not pursued.

### 4.3. *Two Test Problems*

It should be mentioned that the results of Fourier analysis of global errors only applies to problems with periodic boundary conditions. With other forms of boundary conditions, some numerical tests with proper boundary schemes will be necessary. Two simple test problems are tested here with the second-order fully upwind scheme, the third-order upwind-biased scheme and the second-order wavenumber-extended scheme. Both problems are governed by the 1D advection equation. The computational domains for both test problems are $(0, 2\pi)$, which is then discretized with 200-grid intervals. Both the explicit forward time-difference scheme and/or the fourth-order Runge–Kutta time advancing scheme are used for the temporal term. As we are interested primarily in evaluating the spatial formulation, a small Courant number of 0.01 is used in all the calculations to minimize the numerical error from the temporal discretization. All the results shown below will be the solution after 12,800 time steps. All spatial schemes considered here use a five-point stencil.

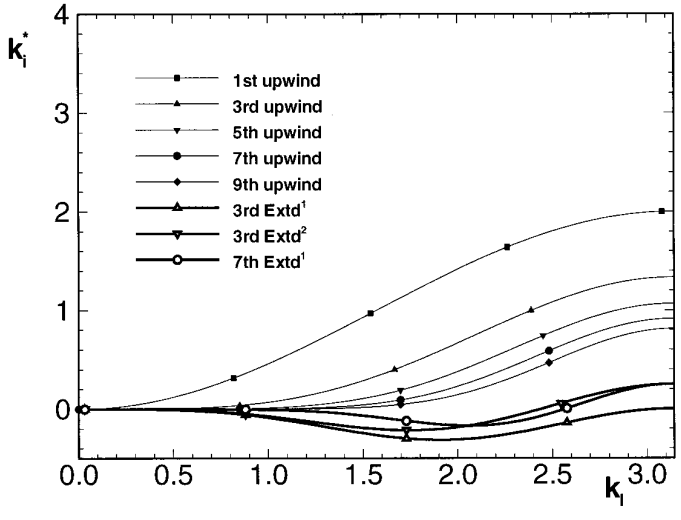


**FIG. 9.** The numerical dissipative errors as indicated by the imaginary part of the modified wavenumber versus wavenumber for different wavenumber-extended upwind-biased finite-difference schemes including a numerical dissipation constraint.

The first test is the propagation of a discontinuity, which contains essentially high-order harmonics. The results are shown in Fig. 10. All the three schemes generate oscillations, due to high-frequency components traveling numerically with different speeds from that of the discontinuity. For the second-order fully upwind scheme, the dominant high-frequency components travel much faster; thus the oscillations occur in front of the discontinuity. For the third-order upwind-biased scheme, these high-frequency components travel much slower and the oscillations occur behind the discontinuity. For the new second-order wavenumber-extended scheme, the oscillations occur both in front of the discontinuity and behind. However, the dominant high-frequency components travel with speeds much closer to that of the discontinuity; thus the oscillations are also much closer to the discontinuity than the other two conventional schemes. The maximum magnitude of the oscillation for the new scheme is much smaller than that of the third-order upwind-biased scheme, and similar to that of the second-order fully upwind scheme. Balancing

the oscillation magnitude and phase shift, the new second-order wavenumber-extended scheme produces a better solution than the other two schemes tested. As mentioned in the Introduction, the FCT flux limiter of Zalesak can be used to eliminate oscillations, which is not shown here.

In order to test a selected value of the wavenumber, the propagation of a sinusoidal wave packet is chosen as the second test problem. We chose two wavenumbers, $\pi/20$ and $\pi/10$. The results are shown in Figs. 11 and 12. For a Courant number of less than 0.04, almost identical results were obtained by both the explicit forward time-difference scheme and the fourth-order Runge–Kutta time advancing scheme. The results shown in Figs. 11 and 12 are for a Courant number of 0.01. These results seem to show that there is almost no error resulting from temporal term discretization. At the low wavenumber, all three schemes produce rather accurate results. Similar to the solutions of the first test problem, some oscillations occur at the slope discontinuity of the sinusoidal wave in the beginning or the end of the wave packet. As the wavenumber increases, the advantages of the second-order wavenumber-extended scheme are clearly seen. The phase shifts of this new scheme for the wavenumbers considered are the minimum in the results of all three schemes, and the prediction of the wave magnitude by the new scheme is also better than that of the other two schemes, including a centered difference scheme. It should be mentioned that the analysis method in Section 3 uses a semidiscrete approximation. To optimize the resolution characteristics of finite-difference schemes, both discretization schemes of the space and time derivatives need to be considered. While this paper considers the upwind-biased schemes for the first-order space derivative, some optimized time discretization schemes have been developed and discussed by Tam and Webb [21].

## 5. FOURIER ANALYSIS OF 2D DISCRETIZATION ERROR

The above analysis applies only when the velocity direction follows the coordinate direction. In this section, isotropy errors of the formulated schemes on a two-dimensional square mesh are analyzed. As in the one-dimensional Fourier analysis, it can be shown that a Fourier representation of $\phi(\bar{s})$ is

$$\phi(\bar{s}) = \sum_{l=0}^{N} \hat{\phi}_l e^{ik_l \bar{s}} \tag{43}$$

or

$$\phi(\bar{x}, \bar{y}) = \sum_{l=0}^{N} \hat{\phi}_l e^{ik_l(\bar{x}\cos\theta + \bar{y}\sin\theta)}, \tag{44}$$

where $\bar{s} = \bar{x}\cos\theta + \bar{y}\sin\theta$ and $\bar{s} = s/\Delta x$, $\bar{x} = x/\Delta x$ and $\bar{y} = y/\Delta x$, $\Delta x$ is the mesh size in both the $x$ and $y$ directions. The exact directional derivation is

$$\frac{\partial \phi}{\partial \bar{s}} = \cos\theta \frac{\partial \phi}{\partial \bar{x}} + \sin\theta \frac{\partial \phi}{\partial \bar{y}} = \sum_{l=0}^{N} ik_l \hat{\phi} e^{ik_l \bar{s}}. \tag{45}$$

If the difference scheme (1) is applied in both the $\bar{x}$ and $\bar{y}$ directions

$$\begin{aligned}\left[\frac{\partial \phi}{\partial \bar{s}}\right]_j &= \cos\theta \left[\frac{\partial \phi}{\partial \bar{x}}\right]_j + \sin\theta \left[\frac{\partial \phi}{\partial \bar{y}}\right]_m \\ &= \cos\theta \left[\sum_{n=1}^{N} a_{-n}\phi_{j-n,m} + a_0\phi_{j,m} + \sum_{n=1}^{N} a_n \phi_{j+n,m}\right] \\ &\quad + \sin\theta \left[\sum_{n=1}^{N} a_{-n}\phi_{j,m-n} + a_0\phi_{j,m} + \sum_{n=1}^{N} a_n \phi_{j,m+n}\right],\end{aligned} \tag{46}$$

where $\bar{x}_{j\pm n} = \pm n$ at $\bar{x}_j = 0$, and $\bar{y}_{m\pm n} = \pm n$ at $\bar{y}_m = 0$. We also have

$$\begin{aligned}\phi_{j\pm n,m}(\bar{x}_{j\pm n}, \bar{y}_m) &= \sum_{l=0}^{N} \hat{\phi}_l e^{ik_l(\bar{x}_{j\pm n}\cos\theta + \bar{y}\sin\theta)} = \sum_{l=0}^{N} \hat{\phi}_l e^{\pm ink_l\cos\theta} \\ \phi_{j,m\pm n}(\bar{x}_j, \bar{y}_{m\pm n}) &= \sum_{l=0}^{N} \hat{\phi}_l e^{ik_l(\bar{x}_j\cos\theta + \bar{y}_{m\pm n}\sin\theta)} \\ &= \sum_{l=0}^{N} \hat{\phi}_l e^{\pm ink_l\sin\theta} \\ \phi_{j,m}(\bar{x}_j, \bar{y}_m) &= \sum_{l=0}^{N} \hat{\phi}_l.\end{aligned} \tag{47}$$

Thus

$$\begin{aligned}\left[\frac{\partial \phi}{\partial \hat{s}}\right]_j &= \cos\theta \sum_{l=0}^{N} \hat{\phi}_l \left(\sum_{n=1}^{N} a_{-n}e^{-ink_l\cos\theta} + a_0 + \sum_{n=1}^{N} a_n e^{ink_l\cos\theta}\right) \\ &\quad + \sin\theta \sum_{l=1}^{N} \hat{\phi}_l \left(\sum_{n=0}^{N} a_{-n}e^{-ink_l\sin\theta} + a_0 + \sum_{n=1}^{N} a_n e^{ink_l\sin\theta}\right) \\ &= \cos\theta \sum_{l=0}^{N} \left(\sum_{n=1}^{N} [(a_n + a_{-n})\cos(nk_l\cos\theta)]\right. \\ &\quad \left. + a_0 + \sum_{n=1}^{N} [(a_n - a_{-n})i\sin(nk_l\cos\theta)]\right) \hat{\phi}_l \\ &\quad + \sin\theta \sum_{l=0}^{N} \left(\sum_{n=1}^{N} [(a_n + a_{-n})\cos(nk_l\sin\theta)]\right. \\ &\quad \left. + a_0 + \sum_{n=1}^{N} [(a_n - a_{-n})i\sin(nk_l\sin\theta)]\right) \hat{\phi}_l;\end{aligned} \tag{48}$$

that is,

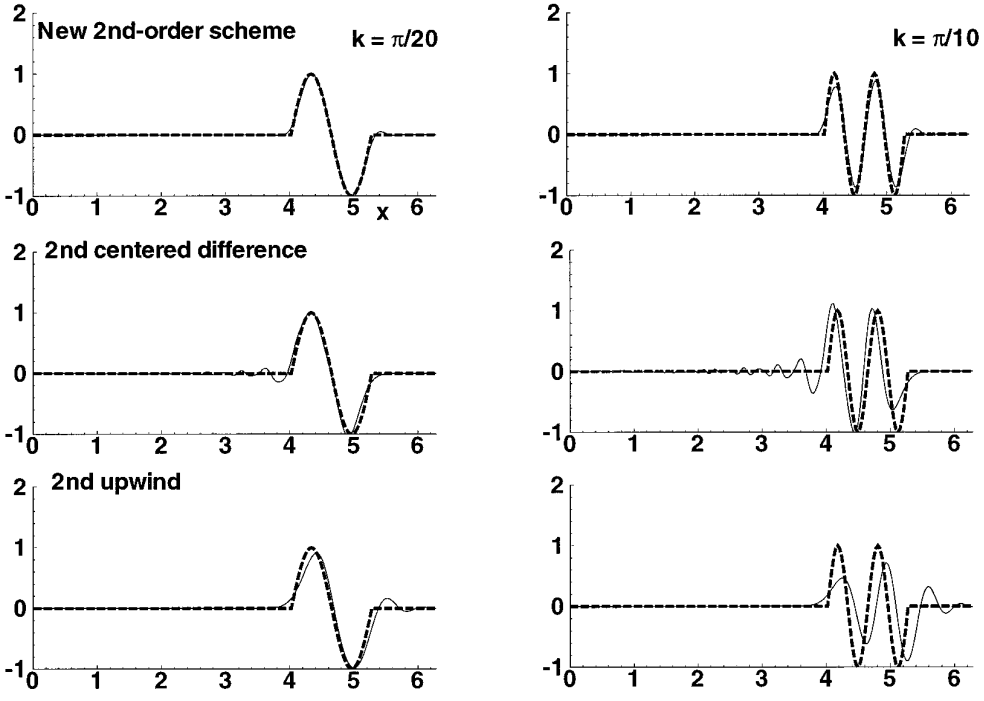


**FIG. 11.** Comparison of three schemes on the linear convection equation for a propagating sinusoidal wave packet for three wavenumbers. The explicit forward time-difference scheme is used. The Courant number is 0.01.

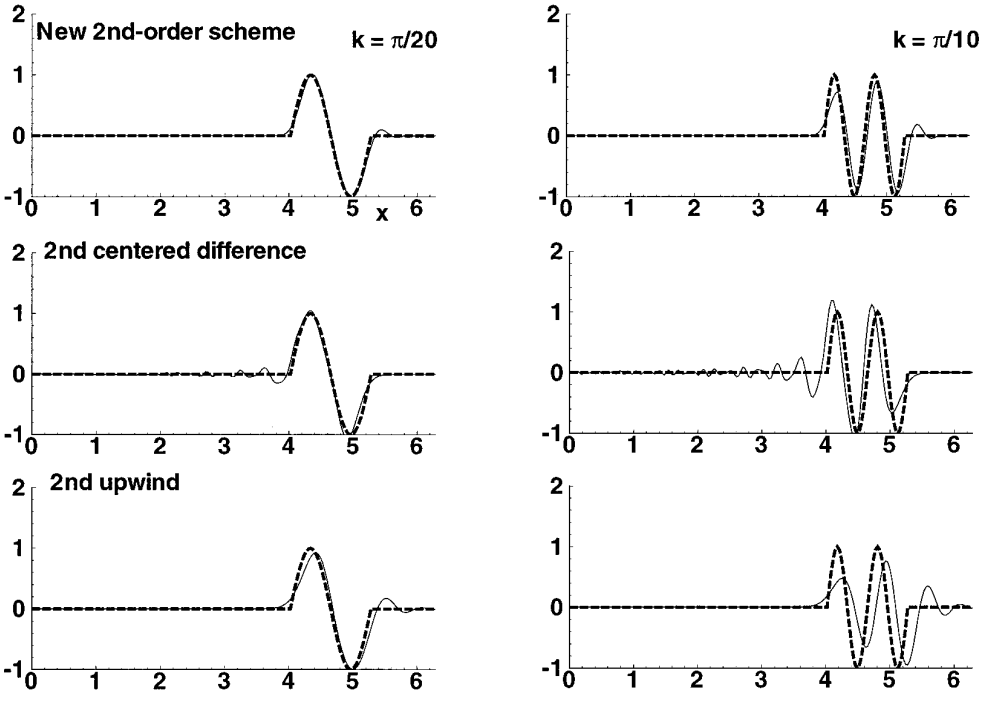


**FIG. 12.** Comparison of three schemes on the linear convection equation for a propagating sinusoidal wave packet for three wavenumbers. The fourth-order Runge–Kutta time advancing method is used. The Courant number is 0.01.

$$\left[\frac{\partial \phi}{\partial \hat{s}}\right]_j = \sum_{l=0}^{N} \left( \cos\theta \left[ \sum_{n=1}^{N} ((a_n + a_{-n}) \cos(nk_l \cos\theta)) + a_0 \right] + \sin\theta \left[ \sum_{n=1}^{N} ((a_n + a_{-n}) \cos(nk_l \sin\theta)) + a_0 \right] \right) \hat{\phi}_l + \sum_{l=0}^{N} \left( \cos\theta \sum_{n=1}^{N} ((a_n - a_{-n}) i \sin(nk_l \cos\theta)) + \sin\theta \sum_{k=1}^{N} ((a_n - a_{-n}) i \sin(nk_l \sin\theta)) \right) \hat{\phi}_l. \tag{49}$$

Comparing the exact solution (45) and the approximation (49), the modified wavenumber $k^*$ in the $s$ coordinate is

$$k_s^* = k_x^* \cos\theta + k_y^* \sin\theta, \tag{50}$$

where

$$\begin{aligned} k_x^* &= \sum_{n=1}^{N} [(a_n - a_{-n}) \sin(nk_l \cos\theta)] - i \left( \sum_{n=1}^{N} [(a_n + a_{-n}) \cos(nk_l \cos\theta)] + a_0 \right) \\ k_y^* &= \sum_{n=1}^{N} [(a_n - a_{-n}) \sin(nk_l \sin\theta)] - i \left( \sum_{n=1}^{N} [(a_n + a_{-n}) \cos(nk_l \sin\theta)] + a_0 \right). \end{aligned} \tag{51}$$

Again, $k^*$ is a complex function. The real part and the imaginary part are associated with the dispersion error and the dissipation error, respectively:

$$\begin{aligned} k_r^* &= \cos\theta \sum_{n=1}^{N} [(a_n - a_{-n}) \sin(nk_l \cos\theta)] + \sin\theta \sum_{n=1}^{N} [(a_n - a_{-n}) \sin(nk_l \sin\theta)] \\ k_i^* &= \cos\theta \left( \sum_{n=1}^{N} [(a_n + a_{-n}) \cos(nk_l \cos\theta)] + a_0 \right) + \sin\theta \left( \sum_{n=1}^{N} [(a_n + a_{-n}) \cos(nk_l \sin\theta)] + a_0 \right). \end{aligned} \tag{52}$$

Again, the coefficient dependence of the real part of the modified wavenumber is only $(a_n - a_{-n})$. Thus, the isotropy error of the dispersion property of the upwind-biased schemes of order $2N - 1$ is the same as that of the centered difference scheme of order $2N$.

Figure 13 plots the ratio between the modified wavenumber and the real wavenumber $(k_r^*/k_l)$ for different upwind-biased schemes. All the schemes are anisotropic. The largest error always occurs along the lines at 0° and 90°. For the low-wavenumber range, e.g., $k_l < \pi/3$, the anisotropy errors become smaller as the order of the schemes becomes higher. However, for high wavenumbers, e.g., $k_l = \pi/2$, the scheme becomes more anisotropic for higher-order schemes.

The wavenumber-extended schemes change the dispersive isotropy error of the upwind-biased schemes very little (see Fig. 14). Generally, for the wavenumber-extended schemes, the isotropy error is improved slightly for the low-wavenumber range, and becomes slightly worse for the high-wavenumber range. The above analysis shows that the waves travel numerically not only with different phase speeds for different wavenumbers, but also with different phase speeds for different directions.

In Figs. 15 and 16, the direction-dependent behaviors of the numerical dissipation are shown. A slightly different numerical dissipation indicator is used. We use $\exp(-k_i^*)$ to indicate the damping of $\hat{\phi}_l(t)$ (see Eq. (36)). The exact solution should be a perfect quarter-circle of radius unity for all wavenumbers. The results show that all the schemes exhibit anisotropic behavior of numerical dissipation, as expected. The largest numerical dissipation for all the upwind schemes (except $k_l = \pi$ for the first-order upwinding scheme) occurs at $\theta = 0°$ or 90°, which first seems to contradict the analyses of de Vahl Davis and Mallinson [25] and Demuren [26]. However, in the analysis of de Vahl Davis and Mallinson [25], it is the cross-stream artificial diffusivity for the first-order upwind scheme which is a maximum at $\theta = 45°$. The analysis here seems to apply only to the streamwise artificial dissipation, which is a maximum at $\theta = 0°$ or 90° and falls to a minimum at $\theta = 45°$. This streamwise artificial dissipation behavior agrees well with the analysis of de Vahl Davis and Mallinson [25]. The anisotropic behavior of numerical dissipation becomes strongest for the high-wavenumber range. The numerical dissipation is very small for the low-wavenumber range for the higher-order schemes. There is a slight reduction in the magnitude of the numerical dissipation indicator for the wavenumber-extended schemes; however, the anisotropy level also worsens slightly.

The numerical dissipation indicator for the schemes 3rd Extd[1], 3rd Extd[2], and 7th Extd[1] behaves as expected, with values larger than unity for some wavenumber ranges (not shown). This indicates that these schemes are not stable.

No attempt is directed at improving the isotropy error, although this may be done by minimizing the angle dependence of expression (52). One possible approach is to use more upwinding diagonal points. This is the idea behind the skew upwinding schemes [27]. Zingg and Lomax [12] optimized the finite-difference schemes on regular triangu-

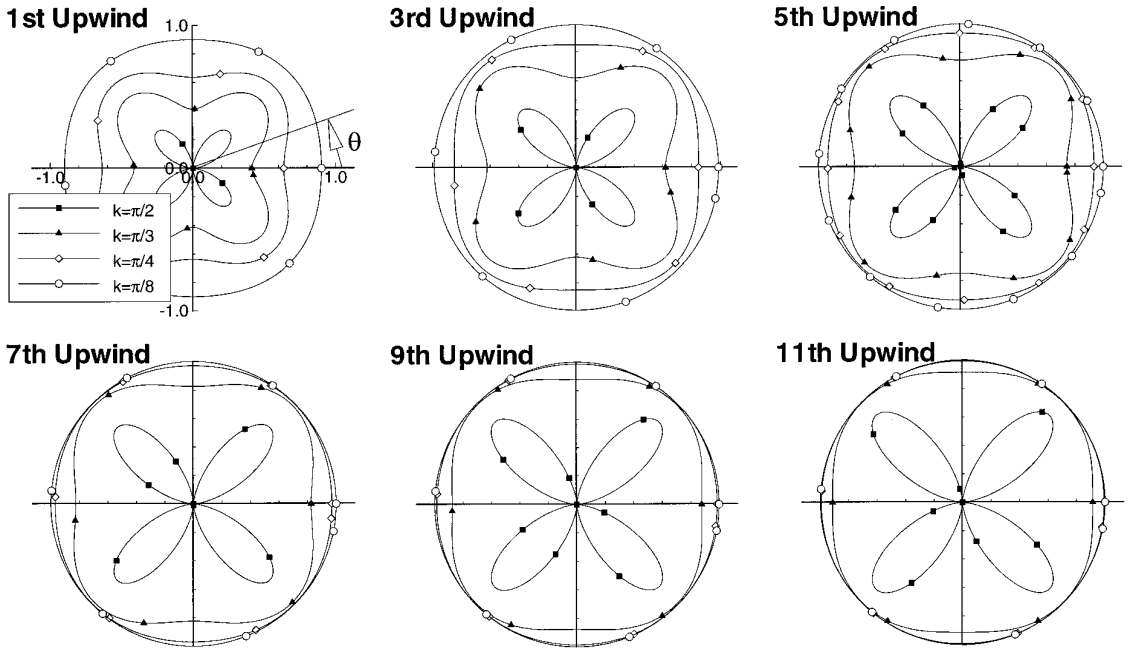


**FIG. 13.** Polar plots of the ratio of numerical phase speed to the exact speed for different upwind-biased finite-difference schemes on a uniform square grid. The phase speeds for four scaled wavenumbers, $\pi/2$, $\pi/2$, $\pi/3$, $\pi/4$, and $\pi/8$, are shown. The two polar coordinates are the ratio of numerical phase speed to the exact speed and the angle of the streamline with respect to the $x$-axis, respectively.

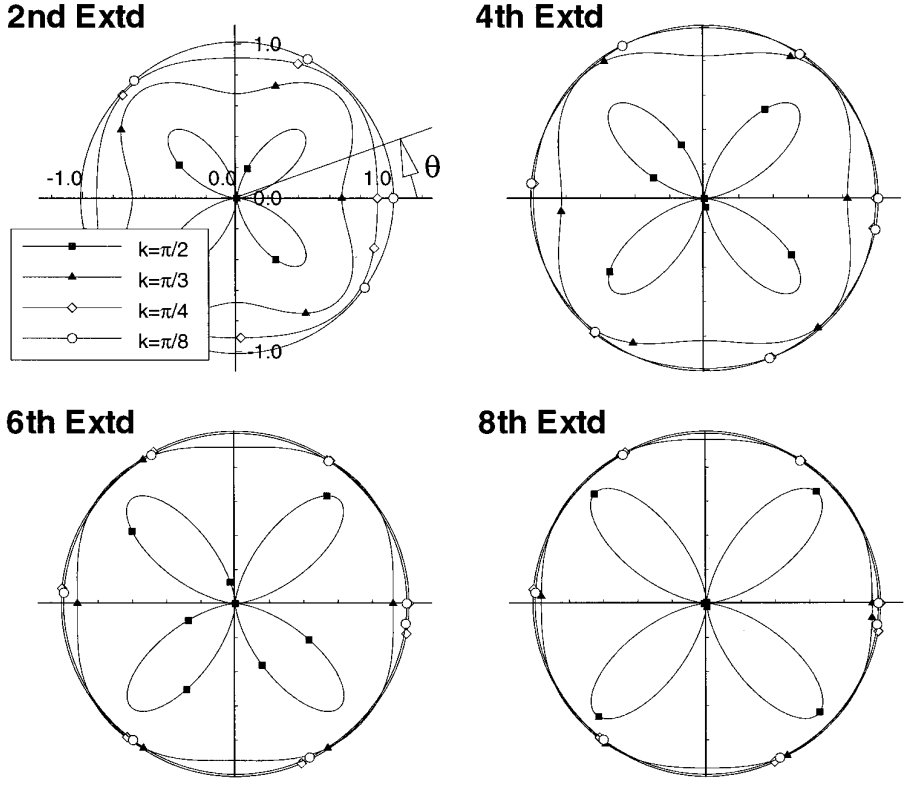


**FIG. 14.** Polar plots of the ratio of numerical phase speed to the exact speed for different wavenumber-extended upwind-biased finite-difference schemes on a uniform square grid. The phase speeds for four scaled wavenumbers, $\pi/2$, $\pi/3$, $\pi/4$, and $\pi/8$, are shown. The two polar coordinates are the ratio of numerical phase speed to the exact speed and the angle of the streamline with respect to the $x$-axis, respectively.

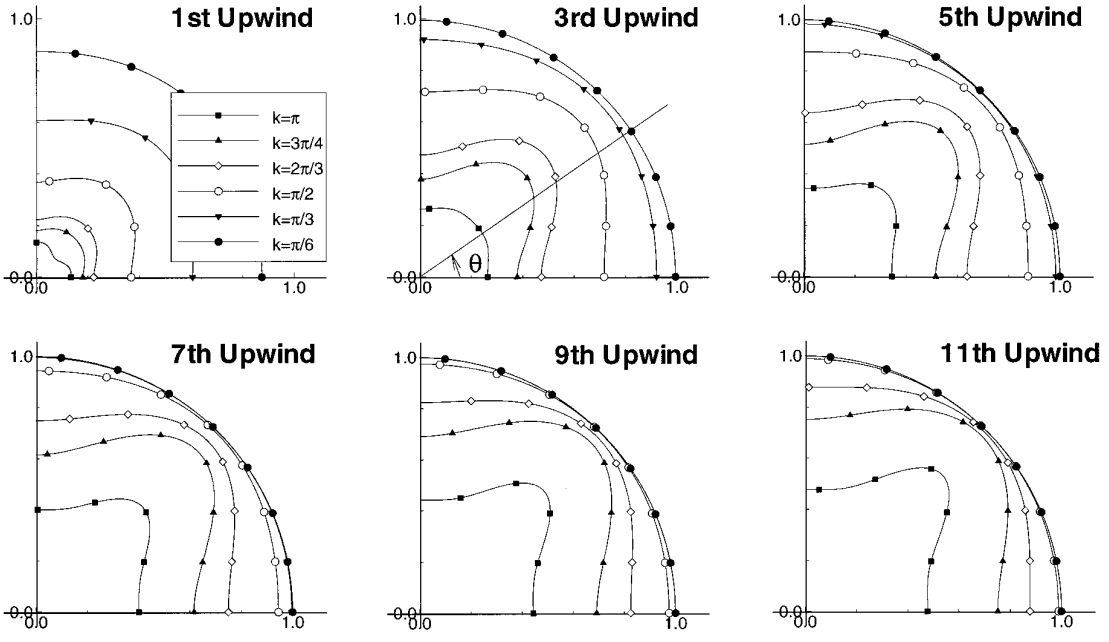


**FIG. 15.** Polar plots of the numerical dissipation indicator for different upwind-biased finite-difference schemes on a uniform square grid. The two polar coordinates are the numerical dissipation indicator and the angle of the streamline with respect to the *x*-axis, respectively.

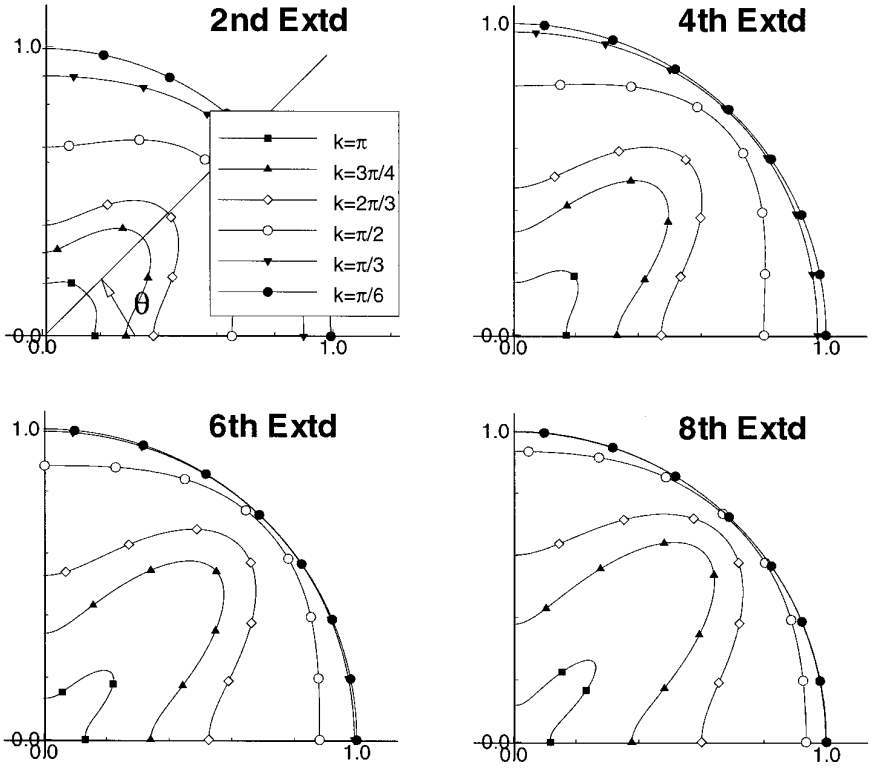


**FIG. 16.** Polar plots of the numerical dissipation indicator for different wavenumber-extended upwind-biased finite-difference schemes on a uniform square grid. The two polar coordinates are the numerical dissipation indicator and the angle of the streamline with respect to the *x*-axis, respectively.

lar grids, which gives six immediate neighbor points for a given node.

## 6. CONCLUSIONS

A number of new wavenumber-extended high-order upwind-biased schemes are presented. These schemes are able to accurately resolve a much larger wavenumber range than the conventional high-order upwind-biased schemes, which is shown by both the Fourier analysis and two test problems. As the formulation of these wavenumber-extended schemes is similar to the second-order or third-order upwind schemes used in current finite-difference and finite-volume CFD codes, the implementation and application of the wavenumber-extended schemes are straightforward. Lele [7] anticipated that in general difference approximations, a lower-order scheme can have better resolution characteristics than a higher-order scheme. The development of the schemes in this paper also confirms this anticipation in the context of high-order upwind-biased schemes.

The new wavenumber-extended high-order upwind-biased schemes are developed by using some additional constraints from the classical Fourier analysis in the scheme construction process. Both the wavenumber- and the direction-dependent dispersion and dissipation characteristics are analyzed for the conventional high-order upwind schemes up to 11th order. The constraints from the Fourier analysis in constructing the wavenumber-extended upwind schemes provide some better overall quantitative control of numerical dispersion and dissipation. The encouraging test results presented in this paper suggest that the developed 2nd- and 4th-order wavenumber-extended upwind-biased schemes provide some alternatives with much better resolution characteristics for replacing the conventional 2nd- or 3rd-order upwind schemes in finite-difference and finite-volume simulations of practical time-dependent flows.

## APPENDIX 1

### A Summary of Upwind-Biased Finite-Difference Schemes

The following upwind-biased finite-difference schemes are derived based on the constraints defined in Eq. (14). The first-order upwind scheme is a special case, but is included here. The schemes are constructed manually by first solving for $a_n - a_{-n}$, and then $a_0$ and $a_n + a_{-n}$. The schemes are also constructed by solving the system of linear equations that resulted from the constraint relations with a simple solver for linear equations. As in some finite-volume formulations, the cell face value of the variable is used and correspondingly their interpolation formulas are also documented here. The schemes will be presented for the case $u_i > 0$ only and those for $u_i < 0$ are analogous to the former.

- *The first-order upwind scheme:*

$$\left(\frac{\partial \phi}{\partial x}\right) = \frac{1}{1!\,\Delta x}(\phi_i - 1!\phi_{i-1}) \tag{53}$$

$$\phi_{i-1/2} = \phi_{i-1}$$

$$\phi_{i+1/2} = \phi_i. \tag{54}$$

- *The third-order upwind-biased scheme:*

$$\left(\frac{\partial \phi}{\partial x}\right) = \frac{1}{3!\,\Delta \mathrm{x}}(\phi_{i-2} - 3!\phi_{i-1} + 3\phi_i + 2\phi_{i+1}) \tag{55}$$

$$\phi_{i-1/2} = \frac{1}{3!}(-\phi_{i-2} + 5\phi_{i-1} + 2\phi_i)$$

$$\phi_{i+1/2} = \frac{1}{3!}(-\phi_{i-1} + 5\phi_i + 2\phi_{i+1}). \tag{56}$$

- *The fifth-order upwind-biased scheme:*

$$\left(\frac{\partial \phi}{\partial x}\right) = \frac{1}{5!\,\Delta x}(-4\phi_{i-3} + 30\phi_{i-2} - 5!\phi_{i-1} + 40\phi_i + 60\phi_{i+1} - 6\phi_{i+2}) \tag{57}$$

$$\phi_{i-1/2} = \frac{1}{5!}(4\phi_{i-3} - 26\phi_{i-2} + 94\phi_{i-1} + 54\phi_i - 6\phi_{i+1})$$

$$\phi_{i-1/2} = \frac{1}{5!}(4\phi_{i-2} - 26\phi_{i-1} + 94\phi_i + 54\phi_{i+1} - 6\phi_{i+2}). \tag{58}$$

This scheme was first formulated by Rai [8]. The scheme has also been used for direct Navier–Stokes solutions [6] and for use with $k - \varepsilon$ turbulence models [9].

- *The seventh-order upwind-biased scheme:*

$$\left(\frac{\partial \phi}{\partial x}\right) = \frac{1}{7!\,\Delta x}(36\phi_{i-4} - 336\phi_{i-3} + 1512\phi_{i-2} - 7!\phi_{i-1} + 1260\phi_i + 3024\phi_{i+1} - 504\phi_{i+2} + 48\phi_{i+3}) \tag{59}$$

$$\phi_{i-1/2} = \frac{1}{7!}(-36\phi_{i-4} + 300\phi_{i-3} - 1212\phi_{i-2} + 3828\phi_{i-1} + 2568\phi_i - 456\phi_{i+1} + 48\phi_{i+2})$$

$$\phi_{i+1/2} = \frac{1}{7!}(-36\phi_{i-3} + 300\phi_{i-2} - 1212\phi_{i-1} + 3828\phi_i + 2568\phi_{i+1} - 456\phi_{i+2} + 48\phi_{i+3}). \tag{60}$$

• *The ninth-order upwind-biased scheme:*

$$\left(\frac{\partial \phi}{\partial x}\right) = \frac{1}{9!\,\Delta x}(-576\phi_{i-5} + 6480\phi_{i-4} - 34{,}560\phi_{i-3} + 120{,}960\phi_{i-2} - 9!\phi_{i-1} + 72{,}576\phi_i + 241{,}920\phi_{i+1} - 51{,}840\phi_{i+2} + 8640\phi_{i+3} - 720\phi_{i+4}) \quad (61)$$

$$\phi_{i-1/2} = \frac{1}{9!}(576\phi_{i-5} - 5904\phi_{i-4} + 28{,}656\phi_{i-3} - 92{,}304\phi_{i-2} + 270{,}576\phi_{i-1} + 198{,}000\phi_i - 43{,}920\phi_{i+1} + 7920\phi_{i+2} - 720\phi_{i+3})$$

$$\phi_{i+1/2} = \frac{1}{9!}(576\phi_{i-4} - 5904\phi_{i-3} + 28{,}656\phi_{i-2} - 92{,}304\phi_{i-1} + 270{,}576\phi_i + 198{,}000\phi_{i+1} - 43{,}920\phi_{i+2} + 7920\phi_{i+3} - 720\phi_{i+4}). \quad (62)$$

• *The 11th-order upwind-biased scheme:*

$$\left(\frac{\partial \phi}{\partial x}\right) = \frac{1}{11!\,\Delta x}(14{,}400\phi_{i-6} - 190{,}080\phi_{i-5} + 1{,}188{,}000\phi_{i-4} - 4{,}752{,}000\phi_{i-3} + 14{,}256{,}000\phi_{i-2} - 11!\phi_{i-1} + 6{,}652{,}800\phi_i + 28{,}512{,}000\phi_{i+1} - 7{,}128{,}000\phi_{i+2} + 1{,}584{,}000\phi_{i+3} - 237{,}600\phi_{i+4} + 17{,}280\phi_{i+5}) \quad (63)$$

$$\phi_{i-1/2} = \frac{1}{11!}(-14{,}400\phi_{i-6} + 175{,}680\phi_{i-5} - 1{,}012{,}320\phi_{i-4} + 3{,}739{,}680\phi_{i-3} - 10{,}516{,}320\phi_{i-2} + 29{,}400{,}480\phi_{i-1} + 22{,}747{,}680\phi_i - 5{,}764{,}320\phi_{i+1} + 1{,}363{,}680\phi_{i+2} - 220{,}320\phi_{i+3} + 17{,}280\phi_{i+4})$$

$$\phi_{i-1/2} = \frac{1}{11!}(-14{,}400\phi_{i-5} + 175{,}680\phi_{i-4} - 1{,}012{,}3204\phi_{i-3} + 3{,}739{,}680\phi_{i-2} - 10{,}516{,}320\phi_{i-1} + 29{,}400{,}480\phi_i + 22{,}747{,}680\phi_{i+1} - 5{,}764{,}320\phi_{i+2} + 1{,}363{,}680\phi_{i+3} - 220{,}320\phi_{i+4} + 17{,}280\phi_{i+5}). \quad (64)$$

Note: 1! = 1, 3! = 6, 5! = 120, 7! = 5040, 9! = 362,880, and 11! = 39,916,800.

## APPENDIX 2

### The Integrated Error Minimization Approach

Substituting the real part of the modified wavenumber, $k_r^*$ (27), into the definition of the integrated error, $E_r$ (39), we obtain

$$E_r = \int_0^{\gamma\pi} \left\{ k - \sum_{n=1}^{N} [(a_n - a_{-n}) \sin(nk_l)] \right\}^2 dk. \quad (65)$$

After some simple algebraic manipulation, the minimum condition of (40) becomes

$$\int_0^{\gamma\pi} \left[ k - \sum_{n=1}^{N} (a_n - a_{-n}) \sin(nk) \right] \sin(Jk)\, dk = 0, \quad J = -N \text{ to } N. \quad (66)$$

Equation (66) provides a system of linear algebraic equations which can be used for additional constraints in deriving the wavenumber-extended schemes. If all the linear algebraic equations in (66) are not used, then a proper choice of $J$ is very important. For the wavenumber-extended upwind-biased schemes of $2N - 2$ formal order, only one equation is needed from (66). Numerical experiments show that $J = -1$ is the best choice.

We take the example of deriving the eighth-order wavenumber-extended upwind-biased scheme to demonstrate the choice of the optimization range factor $\gamma$. In Fig. 17, three optimized schemes are presented for three different $\gamma$ values. The scheme obtained with a large $\gamma$ value of 0.89 produces a considerable deviation of the modified wavenumber from the true wavenumber in the high-wavenumber range starting from intersection point $D$. A small $\gamma$ value of 0.49 is not able to exploit the full potential of the optimized scheme. Although the range of wavenumbers, in

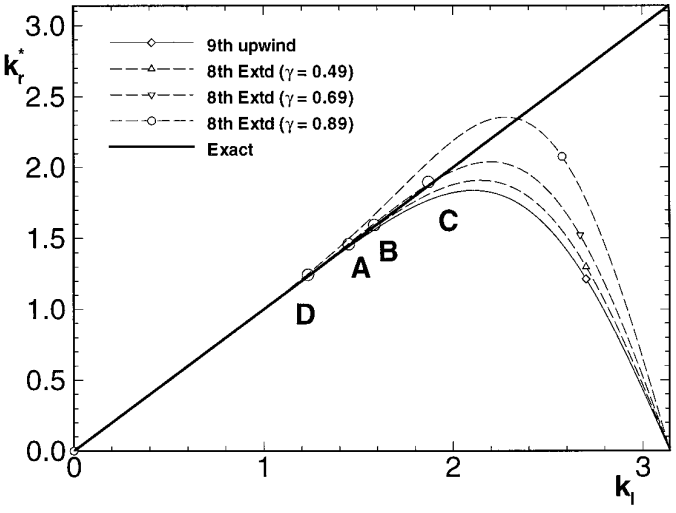


**FIG. 17.** The numerical dissipative errors as indicated by the imaginary part of the modified wavenumber versus wavenumber for three "optimized" upwind-biased finite-difference schemes with different optimization range factor $\gamma$ values.

which the optimized scheme sticks to the exact solution, becomes wider for $\gamma = 0.49$, the overall improvement of the resolution characteristics is still not the optimum. By numerical experiments, a $\gamma$ value of 0.69 was found to be the optimum. Similar experiments were carried out for all other schemes. The following optimum $\gamma$ values were found to give the best results: $\gamma = 0.42$ for $N = 2$, $\gamma = 0.55$ for $N = 3$, $\gamma = 0.65$ for $N = 4$, and $\gamma = 0.69$ for $N = 5$. These $\gamma$ values were used to produce the first class of optimized wavenumber-extended schemes documented in Appendix 3.

A similar integrated error can be defined for the imaginary part of the modified wavenumber

$$E_i = \int_0^{\gamma\pi} (k_i^*)^2 \, dk. \tag{67}$$

Again, substituting the imaginary part of the modified wavenumber, $k_i^*$, into this definition, we obtain

$$E_i = \int_0^{\gamma\pi} \left\{ \sum_{n=1}^{N} [(a_n + a^-_n) \cos(nk_l)] + a_0 \right\}^2 dk. \tag{68}$$

After some simple algebraic manipulation, the minimum condition of $\partial E_i / \partial a_J = 0$ $(-N \le J \le N)$ gives

$$\int_0^{\gamma\pi} \left\{ a_0 + \sum_{n=1}^{N} [(a_n - a_{-n}) \cos(nk)] \right\} \cos(Jk) \, dk = 0. \tag{69}$$

Equation (69) provides another system of linear algebraic equations which can be used for additional constraints in deriving the wavenumber-extended schemes. As discussed in Section 4.2, the schemes obtained by the additional constraints (42) are not stable. The imaginary part of the modified wavenumber becomes negative for some wavenumber ranges. In the schemes obtained by the integrated error minimization approach, this negative wavenumber range is in the relatively low wavenumber end, and in Lele's approach, this negative wavenumber range is in the relatively high wavenumber end. In Appendix 3, the second class of the optimized wavenumber-extended schemes obtained by Lele's approach is documented.

## APPENDIX 3

### A Summary of Wavenumber-Extended Upwind-Biased Finite-Difference Schemes

The *first class* of wavenumber-extended upwind-biased finite-difference schemes are those with constraints (41). In this class of schemes, the wavenumber range with a better dispersion accuracy is extended. As in some finite-volume formulations, the cell face value of the variable is used and correspondingly their interpolation formulas are also documented here. The schemes will be presented for the case $u_i > 0$ only and those for $u_i < 0$ are analogous to the former.

• *The second-order wavenumber-extended upwind-biased scheme:*

$$\left(\frac{\partial \phi}{\partial x}\right) = \frac{1}{\Delta x} (0.213933\phi_{i-2} - 1.141798\phi_{i-1} + 0.641798\phi_i + 0.286067\phi_{i+1}) \tag{70}$$

$$\phi_{i-1/2} = -0.213933\phi_{i-2} + 0.927865\phi_{i-1} + 0.286067\phi_i$$
$$\phi_{i+1/2} = -0.213933\phi_{i-1} + 0.927865\phi_i + 0.286067\phi_{i+1}. \tag{71}$$

• *The fourth-order wavenumber-extended upwind-biased scheme:*

$$\left(\frac{\partial \phi}{\partial x}\right) = \frac{1}{\Delta x} (-0.055453\phi_{i-3} + 0.360600\phi_{i-2} - 1.221201\phi_{i-1} + 0.554534\phi_i + 0.389400\phi_{i+1} - 0.027880\phi_{i+2}) \tag{72}$$

$$\phi_{i-1/2} = 0.055453\phi_{i-3} - 0.305147\phi_{i-2} + 0.916054\phi_{i-1} + 0.361520\phi_i - 0.027880\phi_{i+1}$$
$$\phi_{i+1/2} = 0.055453\phi_{i-2} - 0.305147\phi_{i-1} + 0.916054\phi_i + 0.361520\phi_{i+1} - 0.027880\phi_{i+2}. \tag{73}$$

• *The sixth-order wavenumber-extended upwind-biased scheme:*

$$\left(\frac{\partial \phi}{\partial x}\right) = \frac{1}{\Delta x} (0.015825\phi_{i-4} - 0.127442\phi_{i-3} + 0.482326\phi_{i-2} - 1.303877\phi_{i-1} + 0.553877\phi_i + 0.417674\phi_{i+1} - 0.039225\phi_{i+2} + 0.000842\phi_{i+3}) \tag{74}$$

$$\phi_{i-1/2} = -0.015825\phi_{i-4} + 0.111617\phi_{i-3} - 0.370709\phi_{i-2} + 0.933168\phi_{i-1} + 0.379291\phi_i - 0.038383\phi_{i+1} + 0.000842\phi_{i+2}$$
$$\phi_{i+1/2} = -0.015825\phi_{i-3} + 0.111617\phi_{i-2} - 0.370709\phi_{i-1} + 0.933168\phi_i + 0.379291\phi_{i+1}. - 0.038383\phi_{i+2} - 0.000842\phi_{i+3}. \tag{75}$$

• *The eighth-order wavenumber-extended upwind-biased scheme:*

$$\left(\frac{\partial \phi}{\partial x}\right) = \frac{1}{\Delta x}(-0.004191\phi_{i-5} + 0.041288\phi_{i-4} - 0.188962\phi_{i-3} + 0.552022\phi_{i-2} - 1.328033\phi_{i-1} + 0.528033\phi_i + 0.447978\phi_{i+1} - 0.049133\phi_{i+2} + 0.000379\phi_{i+3} + 0.000619\phi_{i+4}) \quad (76)$$

$$\phi_{i-1/2} = 0.004191\phi_{i-5} - 0.037097\phi_{i-4} + 0.151864\phi_{i-3} - 0.400158\phi_{i-2} + 0.927875\phi_{i-1} + 0.399842\phi_i - 0.048136\phi_{i+1} + 0.000998\phi_{i+2} + 0.000619\phi_{i+3}$$

$$\phi_{i+1/2} = 0.004191\phi_{i-4} - 0.037097\phi_{i-3} + 0.151864\phi_{i-2} - 0.400158\phi_{i-1} + 0.927875\phi_i + 0.399842\phi_{i+1} - 0.048136\phi_{i+2} + 0.000998\phi_{i+3} + 0.000619\phi_{i+4}. \quad (77)$$

The *second class* of the wavenumber-extended upwind-biased finite-difference schemes are those with constraints (42). In this class of schemes, the wavenumber range with a better dispersion accuracy is extended and the numerical dissipation at a certain wavenumber is also specified. These schemes are not stable.

• *The third-order wavenumber-extended upwind-biased scheme 1:*

$k_{l1} = 1.7$, $k_{l2} = 3.1$, $c_2 = 0.0$, and $N = 3$

$$\left(\frac{\partial \phi}{\partial x}\right) = \frac{1}{\Delta x}(-0.066313\phi_{i-2} + 0.282329\phi_{i-2} - 0.799522\phi_{i-1} - 0.132282\phi_i + 0.865376\phi_{i+1} - 0.149589\phi_{i+2}) \quad (78)$$

$$\phi_{i-1/2} = 0.066313\phi_{i-3} - 0.216016\phi_{i-2} + 0.583505\phi_{i-1} + 0.715787\phi_i - 0.149589\phi_{i+1}$$

$$\phi_{i+1/2} = 0.066313\phi_{i-2} - 0.216016\phi_{i-1} + 0.583505\phi_i + 0.715787\phi_{i+1} - 0.149589\phi_{i+2}. \quad (79)$$

• *The third-order wavenumber-extended upwind-biased scheme 2:*

$k_{l1} = 1.7$, $k_{l2} = 3.1$, $c_2 = 0.25$, and $N = 3$

$$\left(\frac{\partial \phi}{\partial x}\right) = \frac{1}{\Delta x}(-0.066313\phi_{i-2} + 0.297968\phi_{i-2} - 0.862076\phi_{i-1} - 0.038451\phi_i + 0.802822\phi_{i+1} - 0.133950\phi_{i+2}) \quad (80)$$

$$\phi_{i-1/2} = 0.066313\phi_{i-3} - 0.231655\phi_{i-2} + 0.630421\phi_{i-1} + 0.668872\phi_i - 0.1339550\phi_{i+1}$$

$$\phi_{i+1/2} = 0.066313\phi_{i-2} - 0.231655\phi_{i-1} + 0.630421\phi_i + 0.668872\phi_{i+1} - 0.133950\phi_{i+2}. \quad (81)$$

• *The seventh-order wavenumber-extended upwind-biased scheme 1*:

$k_{l1} = 2.2$, $k_{l2} = 3.1$, $c_2 = 0.25$, and $N = 5$

$$\left(\frac{\partial \phi}{\partial x}\right) = \frac{1}{\Delta x}(-0.006146\phi_{i-5} + 0.047576\phi_{i-4} - 0.168880\phi_{i-3} + 0.399623\phi_{i-2} - 0.941121\phi_{i-1} - 0.017192\phi_i + 0.917003\phi_{i+1} - 0.295376\phi_{i+2} + 0.073247\phi_{i+3} - 0.008734\phi_{i+4}) \quad (82)$$

$$\phi_{i-1/2} = 0.006146\phi_{i-5} - 0.041430\phi_{i-4} + 0.127450\phi_{i-3} - 0.272173\phi_{i-2} + 0.668949\phi_{i-1} + 0.686140\phi_i - 0.230863\phi_{i+1} + 0.064514\phi_{i+2} - 0.008734\phi_{i+3}$$

$$\phi_{i+1/2} = 0.006146\phi_{i-4} - 0.041430\phi_{i-3} + 0.127450\phi_{i-2} - 0.272173\phi_{i-1} + 0.668949\phi_i + 0.686140\phi_{i+1} - 0.230863\phi_{i+2} + 0.064514\phi_{i+3} - 0.008734\phi_{i+4}. \quad (83)$$

## ACKNOWLEDGMENTS

The author is grateful to the anonymous reviewers for their useful comments.

## REFERENCES

1. R. F. Warming and R. M. Beam, Upwind second-order difference schemes and applications in aerodynamics flows, *AIAA J.* **14,** 1241 (1976).
2. W. Shyy, A study of finite difference approximations to steady-state, convection-dominated flow problems, *J. Comput. Phys.* **57,** 415 (1985).
3. B. P. Leonard, A stable and accurate convective modelling procedure based on quadratic upstream interpolation, *Comput. Methods Appl. Mech. Eng.* **19,** 59 (1979).
4. A. Harten, High resolution schemes for hyperbolic conservation laws, *J. Comput. Phys.* **49,** 357 (1983).
5. B. P. Leonard, Simple high-accuracy resolution program for convective modeling of discontinuities, *Int. J. Numer. Methods Fluids* **8,** 1291 (1988).
6. M. N. Rai and P. Moin, Direct simulations of turbulent flow using finite-difference schemes, *J. Comput. Phys.* **96,** 15 (1991).
7. S. K. Lele, Compact finite difference schemes with spectral-like resolution, *J. Comput. Phys.* **103,** 16 (1992).

8. M. N. Rai, Navier–Stokes simulations of blade–vortex interaction using high-order accurate upwind schemes, AIAA Paper 87-0543 (1987) (unpublished).
9. P. Tamamidis and D. N. Assanis, Three-dimensional incompressible flow calculations with alternative discretization schemes, *Numer. Heat Transfer B* **24,** 57 (1993).
10. T. Kawamura and K. Kuwahara, Computation of high Reynolds number flow around a circular cylinder with surface roughness, AIAA Paper 84-0340 (1984).
11. R. Vichnevetsky and F. De Schutter, in *Advances in Computer Methods for Partial Differential Equations*, edited by R. Vichnevetsky (AICA/IMACS, Rutgers University, NJ, 1975), p. 46.
12. D. W. Zingg and H. Lomax, Finite-difference schemes on regular triangular grids, *J. Comput. Phys.* **108,** 306 (1993).
13. T. Hayase, A. C. Humphfrey, and R. Grief, A consistently formulated QUICK scheme for fast and stable convergence using finite-volume iterative calculation procedures, *J. Comput. Phys.* **98,** 108 (1992).
14. P. K. Khosla and S. G. Rubin, A diagonally dominant second-order accurate implicit scheme, *Comput. Fluids* **2,** 207 (1974).
15. Y. Li and L. Baldacchino, Implementation of some higher-order convection schemes on non-uniform grids, *Int. J. Numer. Methods Fluids* **21,** 1201 (1995).
16. B. Gustafsson, The convergence rate for difference approximations to mixed initial boundary value problems, *Math. Comput.* **29,** 396 (1975).
17. M. H. Carpenter, D. Gottlieb, and S. Abarbanel, The stability of numerical boundary treatments for compact high-order finite-difference schemes, *J. Comput. Phys.* **108,** 272 (1993).
18. J. C. Strikwerda, Initial boundary value problems for the method of lines, *J. Comput. Phys.* **34,** 94 (1980).
19. S. T. Zalesak, Fully multidimensional flux-corrected transport algorithms for fluids, *J. Comput. Phys.* **31,** 335 (1979).
20. Y. Li and M. Rudman, Assessment of higher-order upwind schemes incorporating FCT for convection-dominated problems, *Numer. Heat Transfer B* **27,** 1 (1995).
21. C. K. W. Tam and J. C. Webb, Dispersion-relation-preserving finite difference schemes for computational acoustics, *J. Comput. Phys.* **107,** 262 (1993).
22. C. A. J. Fletcher, *Computational Techniques for Fluid Dynamics* (Springer-Verlag, Berlin, 1991), Vol. 1.
23. R. Vichnevetsky and J. B. Bowles, *Fourier Analysis of Numerical Approximations of Hyperbolic Equations* (SIAM, Philadelphia, 1982).
24. L. N. Trefethen, Stability of hyperbolic finite-difference models with one or two boundaries, in *Large-Scale Computations in Fluid Mechanics,* edited by B. E. Engquist, S. Osher and R. C. Somerville, Lectures in Applied Mathematics, Vol. 22 (Am. Math Soc., Providence, RI, 1985), p. 311 (1985).
25. G. de Vahl Davis and G. D. Mallinson, An evaluation of upwind and central difference approximations by a study of recirculating flow, *Computers and Fluids* **4**, 29 (1976).
26. A. O. Demuren, False diffusion in three-dimensional flow calculations, *Computer and Fluids* **13**, 411 (1985).
27. G. D. Raithby, Skew upstream differencing schemes for problems involving fluid flow, *Comp. Meths. Appl. Mech. Eng.* **9**, 153 (1976).